Steel and Composite Structures, *Vol. 33, No. 2* (*2019*) *163-180*
DOI: https://doi.org/10.12989/scs.2019.33.2.163

Free vibration analysis of uniform and stepped functionally graded circular cylindrical shells

Haichao Li*, Fuzhen Pang [a], Yuan Du [b] and Cong Gao [c]

College of Shipbuilding Engineering, *Harbin Engineering University*, *Harbin*, *150001*, *P.R. China*

(*Received August 20, 2018, Revised September 28, 2019, Accepted October 13, 2019*)

Abstract. A semi analytical method is employed to analyze free vibration characteristics of uniform and stepped functionally graded circular cylindrical shells under complex boundary conditions. The analytical model is established based on multi-segment partitioning strategy and first-order shear deformation theory. The displacement functions are handled by unified Jacobi polynomials and Fourier series. In order to obtain continuous conditions and satisfy complex boundary conditions, the penalty method about spring technique is adopted. The solutions about free vibration behavior of functionally graded circular cylindrical shells were obtained by approach of Rayleigh–Ritz. To confirm the dependability and validity of present approach, numerical verifications and convergence studies are conducted on functionally graded cylindrical shells under various influencing factors such as boundaries, spring parameters *et al*. The present method apparently has rapid convergence ability and excellent stability, and the results of the paper are closely agreed with those obtained by FEM and published literatures.

Keywords: uniform and stepped functionally graded circular cylindrical; free vibration; multi-segment partitioning strategy; penalty method; complex boundary conditions

1. Introduction

The functionally graded (FG) circular cylindrical shells are widely used in practical engineering applications due to the special self-structural performance and excellent mechanical properties. And the FG circular cylindrical shells are usually working in complex environmental conditions and exposed to a variety of dynamic excitations as results that the excessive vibration. Thus, the vibration characteristics analysis of FG circular cylindrical shells is of great significant. This paper aims to use a semi analytical method to present a unified formulation to analyze the free vibration characteristics of uniform and stepped FG circular cylindrical shells with complex boundary conditions.

In the past few decades, a large number of analytical and numerical methods have been proposed to analyze the vibration characteristics of functionally graded circular cylindrical shells: Tornabene (2009) studied the vibration behavior of FG conical, cylindrical and other structures by using differential quadrature method. Fantuzzi *et al*. (2016) investigated the free vibration of simply supported functionally graded material (FGM) shells, in which spherical and cylindrical shell geometries are included. Brischetto *et al*. (2016) investigated the differences between a three-dimensional (3D) exact solution and several two-dimensional (2D) numerical solutions to analyze the free vibration of functionally graded plates and cylinders. Zghal *et al*. (2018) made comparison study on various FG composite shells reinforced by carbon nanotubes and highlight the efficiency and applicability of the model in forecasting the vibration behavior of the shells. Tornabene and Viola (2009) studied the dynamic behavior of FG circular panels, parabolic panels and shells of revolution based on First-order Shear Deformation Theory. Qu *et al*. (2013b) proposed a unified formulation for vibration analysis of functionally graded shells of revolution with arbitrary boundary conditions. Bidgoli *et al*. (2015) analyzed the instability and nonlinear for vibration of a FG cylindrical shell by using a semi analytical method. Wang *et al*. (2017b) applied the Fourier-Ritz method to study the vibration behavior of the moderately thick functionally graded (FG) parabolic and circular panels and shells of revolution with general boundary conditions. The modified Fourier series is chosen as the basis function of the admissible functions of the structure to eliminate all the relevant discontinuities of the displacements and their derivatives at the edges, and the vibration behavior is solved by means of the Ritz method. Liu *et al*. (2018) analyzed the free vibration characteristics of FG reinforced composite cylindrical shell on the base of three dimensional elasticity theory. Kar and Panda (2015) proposed a nonlinear mathematical model by using higher order shear deformation theory for shallow shell and investigated nonlinear vibration behaviour of FG spherical shells. Beni *et al*. (2015) developed a size-dependent equation to analyze the free vibration behavior of FG cylindrical shell subject to non-classical boundary conditions. In the same field, Zeighampour and Shojaeian (2017) also analyzed the

*Corresponding author, Ph.D.,
E-mail: lihaichao@hrbeu.edu.cn
[a] Professor, E-mail: pangfuzhen@hrbeu.edu.cn
[b] Ph.D. Student, E-mail: duyuan@hrbeu.edu.cn
[c] Ph.D. Student, E-mail: conggao@hrbeu.edu.cn

http://www.techno-press.org/?journal=scs&subpage=6
ISSN: 1229-9367 (Print), 1598-6233 (Online)

FG cylindrical shell vibration with size-dependent. Su *et al*. (2014) presented a unified solution to obtain the vibration characteristics of FG cylindrical and other shell structures. Jin *et al*. (2014) proposed the Haar wavelet method to study the free vibration behavior of FG cylindrical shells, in which the classical first order shear deformation theory is adopted. Wang *et al*. (2017b) also investigated the FG cylindrical shell on base of shear deformation theory, and the differences between this article with other published literatures are the shell structure and the basic theory. Cao and Tang (2012) modified the 3-D foundational equations into coupling 2-D equations, in which the various coefficients were changed into the constant coefficients. Zhang *et al*. (2015) firstly proposed the four-unknown shear deformation theory, and the theory is capable of analyzing the vibration of FG cylindrical shell, including only four independent displacement functions. Zhao *et al*. (2009) used the element-free-kp-method to study the vibration characteristics of FG cylindrical shell, in which the FG shell structure is consist of the metal and ceramic. Ye *et al*. (2016) used the improved Fourier Series method to study the vibration characteristic of FG deep open cylindrical shell. Yas *et al*. (2013) used the differential quadrature approach to investigate the three-dimensional free vibration of FG cylindrical panel subject to simply support at four ends of the structure. Bodaghi and Shakeri (2012) studied not only the free vibration of FG cylindrical panels, but also the transient vibration of the structure by an analytical method, and the shell is acted by impulsive loads with simply support restraints. So the solution of this paper could be used as the reference data for related studies. Hosseini-Hashemi *et al*. (2012) obtained the exact solution of FG cylindrical structure by using Donnell and Sanders theories. Kamarian *et al*. (2014) focused on the vibration behavior of FG sandwich cylindrical shells, and the most significant of this paper is the Pasternak foundation, which make the solution more accurate. Razavi *et al*. (2017) investigated the free vibration characteristics of FG cylindrical shell subject to general restraints at the end of shell structure.

For the vibration analysis of the stepped functionally graded structures, Hosseini-Hashemi *et al*. (2013) used an accurate mathematical method to study free vibration of stepped thickness circular/annular Mindlin functionally graded plates. Javed *et al*. (2016) analyzed the vibration behavior of composite cylindrical shells under non-uniform thickness walls. Bambill *et al*. (2015) studied free transverse vibrations of axially functionally graded beams with stepped changes in geometry and in material properties, in which the differential quadrature method with domain decomposition technique is used, and the governing equations of motion are based on Timoshenko beam theory and are derived using Hamilton's principle. Li *et al*. (2019) used a semi analytical method to analyze free vibration characteristics of uniform and stepped FG shells of revolution. Tang *et al*. (2017) analyzed the vibration characteristics by using reverberation-ray matrix method.

As we can see from the literatures review, researches around the world mainly used analytical method, numerical method, differential quadrature method, Fourier-Ritz method, Haar wavelet method and Modified Fourier-Ritz method et al. to investigate the vibration characteristics of FG cylindrical panels and shells under classical or general boundaries conditions. In addition, we can see that there are rarely any published literatures focused on the vibration analysis of stepped FG cylindrical shell. Therefore, it is of great significant to establish a unified formulation to study free vibration characteristics of uniform and stepped FG circular cylindrical shells subject to complex boundary conditions.

2. Theoretical formulations

2.1 The model description

The model of FG circular cylindrical shell is described in Fig. 1. It is assumed that the FG circular cylindrical shell is made up of same materials. The length of the FG circular cylindrical shell is L. h_i represents the thicknesses of different section for circular cylindrical shell. The model is described by cylindrical coordinate system (x, θ, z), in which the axial and circumferential directions were represented by x and θ, respectively. The displacements in the direction of x, θ, z of the middle surface are respectively represented by u, v and w. The displacement components of FG circular cylindrical shells with reference to its coordinate system are presented as U, V, W. To obtain more accurate results the FG circular cylindrical shells are decomposed into H shell segments along the axial direction (Qu *et al*. 2013b, Pang *et al*. 2019c).

2.2 Functionally graded (FG) model

Two types of FG model are considered and the Voigt's rule is employed to evaluate the effective material properties of layers varying continuously and smoothly in thickness direction in this paper. The Young's modulus (E), mass density (ρ) and Poisson's ratios (ν) of FG model can be expressed as follows

$$E(z) = (E_c - E_m)V_c + E_m \tag{1a}$$

$$\rho(z) = (\rho_c - \rho_m)V_c + \rho_m \tag{1b}$$

$$\nu(z) = (\nu_c - \nu_m)V_c + \nu_m \tag{1c}$$

where the subscripts c and m represent the ceramic and metallic constituents, respectively, and the volume fraction V_c follows two general four-parameter power-law distributions

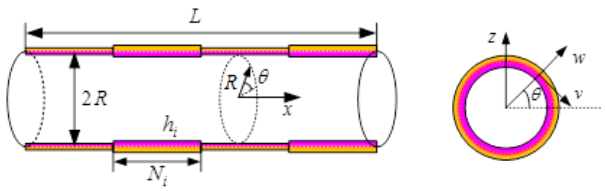

(a) Cross section (b) Differential element

Fig. 1 Geometry notations and coordinate system of FG circular cylindrical shell

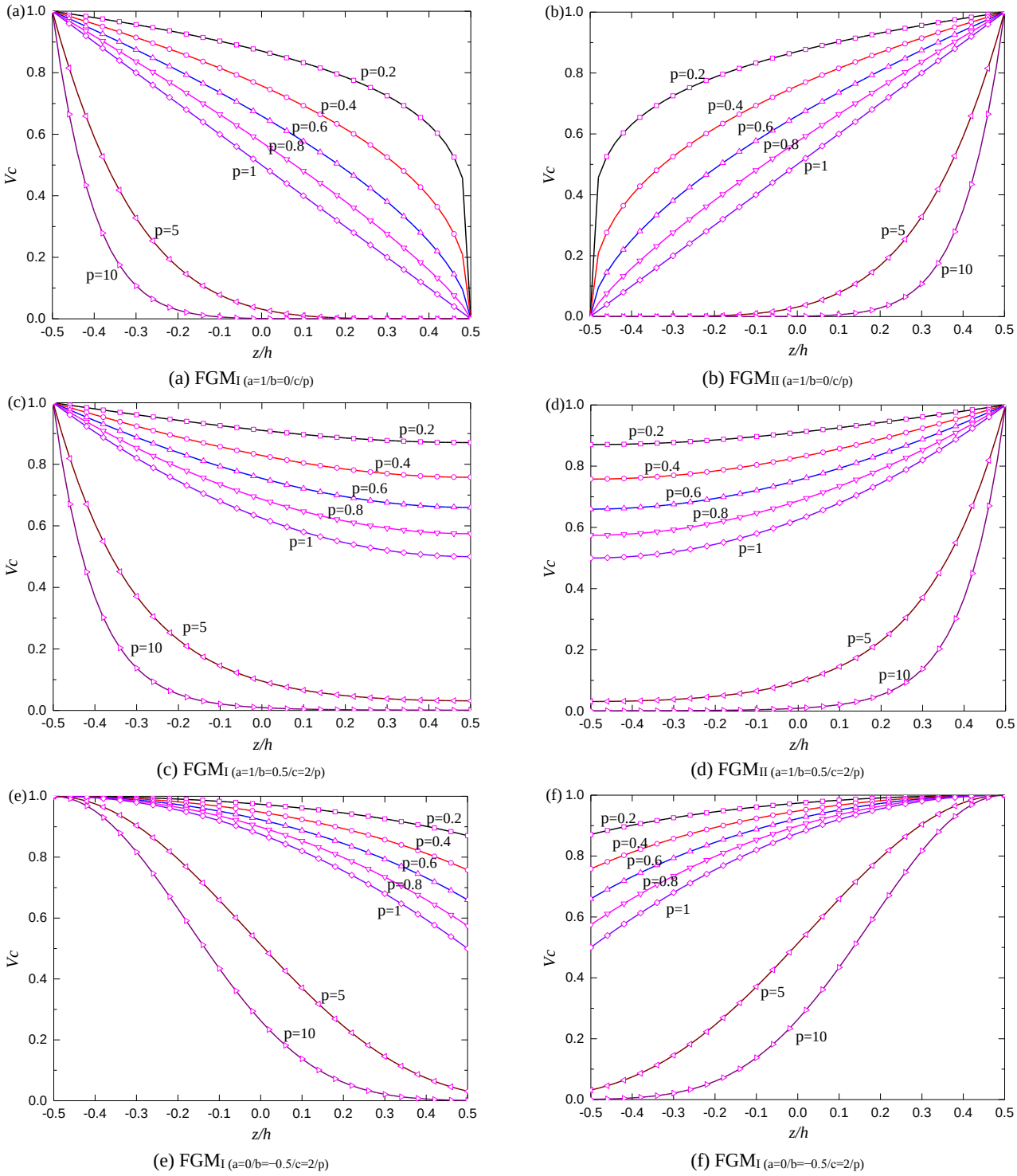

(a) $FGM_{I\,(a=1/b=0/c/p)}$ (b) $FGM_{II\,(a=1/b=0/c/p)}$

(c) $FGM_{I\,(a=1/b=0.5/c=2/p)}$ (d) $FGM_{II\,(a=1/b=0.5/c=2/p)}$

(e) $FGM_{I\,(a=0/b=-0.5/c=2/p)}$ (f) $FGM_{I\,(a=0/b=-0.5/c=2/p)}$

Fig. 2 Variations of the volume fraction (Vc) through the structure thickness for different values of power-law exponent

$$FGM_{I(a/b/c/p)}: V_c = \left[1 - a\left(\frac{1}{2} + \frac{z}{h}\right) + b\left(\frac{1}{2} + \frac{z}{h}\right)^c\right]^p \quad (2a)$$

$$FGM_{II(a/b/c/p)}: V_c = \left[1 - a\left(\frac{1}{2} - \frac{z}{h}\right) + b\left(\frac{1}{2} - \frac{z}{h}\right)^c\right]^p \quad (2b)$$

where p is the power-law exponent and takes only positive values. z signifies the thickness coordinate. The parameters a, b and c determine the material variation profile through functionally graded shell thickness. The different power-law distributions can be obtained by setting proper value of the parameters a, b, c and p. The variations of volume fraction V_c for different values of the parameters a, b, c and p are depicted in Fig. 2

2.3 Energy functions of FG circular cylindrical shell

According to first-order shear deformation shown in Refs. (Wang *et al*. 2017b, Pang *et al*. 2019a, b, Li *et al*.

2019), the strains at any point on FG circular cylindrical shells can be defined in terms of the reference surface displacements and rotations of normal as

$$\varepsilon_x^i = \varepsilon_x^{0,i} + z\kappa_x^{0,i} \qquad \varepsilon_\theta^i = \varepsilon_\theta^{0,i} + z\kappa_\theta^{0,i} \tag{3a}$$

$$\gamma_{x\theta}^i = \gamma_{x\theta}^{0,i} + z\kappa_{x\theta}^{0,i} \qquad \gamma_{xz}^i = \gamma_{xz}^{0,i} \qquad \gamma_{\theta z}^i = \gamma_{\theta z}^{0,i} \tag{3b}$$

Meanwhile, the membrane strains can also be obtained in mentioned Refs (Wang *et al*. 2017b, Pang *et al*. 2019a, b, Li *et al*. 2019). Based on the law of Hook, the stresses can be described as below

$$\begin{Bmatrix} \sigma_x^i \\ \sigma_\theta^i \\ \tau_{x\theta}^i \\ \tau_{xz}^i \\ \tau_{\theta z}^i \end{Bmatrix} = \begin{bmatrix} Q_{11}(z) & Q_{12}(z) & 0 & 0 & 0 \\ Q_{12}(z) & Q_{22}(z) & 0 & 0 & 0 \\ 0 & 0 & Q_{66}(z) & 0 & 0 \\ 0 & 0 & 0 & Q_{66}(z) & 0 \\ 0 & 0 & 0 & 0 & Q_{66}(z) \end{bmatrix} \begin{Bmatrix} \varepsilon_x^i \\ \varepsilon_\theta^i \\ \gamma_{x\theta}^i \\ \gamma_{xz}^i \\ \gamma_{\theta z}^i \end{Bmatrix} \tag{4}$$

where σ_x^i and σ_θ^i are normal stresses; $\tau_{x\theta}^i$, τ_{xz}^i and $\tau_{\theta z}^i$ denote shear stresses. ε_x^i and ε_θ^i are normal strains in the direction of x and θ. $\gamma_{x\theta}$ is shear strains. $Q_{ij}(z)$ (i, j = 1, 2, 6) are constants, and the value of which are obtained as displayed in Eq. (5)

$$Q_{11}(z) = \frac{E(z)}{1-\nu^2(z)}, \quad Q_{12}(z) = \frac{\nu(z)E(z)}{1-\nu^2(z)}, \quad Q_{66}(z) = \frac{E(z)}{2[1+\nu(z)]} \tag{5}$$

By carrying the integration of the stresses over the cross-section, the force and moment resultants can be obtained as follows

$$\begin{Bmatrix} N_x^i \\ N_\theta^i \\ N_{x\theta}^i \end{Bmatrix} = \begin{bmatrix} A_{11} & A_{12} & 0 \\ A_{12} & A_{22} & 0 \\ 0 & 0 & A_{66} \end{bmatrix} \begin{Bmatrix} \varepsilon_x^{0,i} \\ \varepsilon_\theta^{0,i} \\ \gamma_{x\theta}^{0,i} \end{Bmatrix} + \begin{bmatrix} B_{11} & B_{12} & 0 \\ B_{12} & B_{22} & 0 \\ 0 & 0 & B_{66} \end{bmatrix} \begin{Bmatrix} \varepsilon_x^{0,i} \\ \varepsilon_\theta^{0,i} \\ \gamma_{x\theta}^{0,i} \end{Bmatrix} \tag{6a}$$

$$\begin{Bmatrix} M_x^i \\ M_\theta^i \\ M_{x\theta}^i \end{Bmatrix} = \begin{bmatrix} B_{11} & B_{12} & 0 \\ B_{12} & B_{22} & 0 \\ 0 & 0 & B_{66} \end{bmatrix} \begin{Bmatrix} \varepsilon_x^{0,i} \\ \varepsilon_\theta^{0,i} \\ \gamma_{x\theta}^{0,i} \end{Bmatrix} + \begin{bmatrix} D_{11} & D_{12} & 0 \\ D_{12} & D_{22} & 0 \\ 0 & 0 & D_{66} \end{bmatrix} \begin{Bmatrix} \kappa_x^i \\ \kappa_\theta^i \\ \kappa_{x\theta}^i \end{Bmatrix} \tag{6b}$$

$$\begin{Bmatrix} Q_x^i \\ Q_\theta^i \end{Bmatrix} = \bar{\kappa} \begin{bmatrix} A_{66} & 0 \\ 0 & A_{66} \end{bmatrix} \begin{bmatrix} \gamma_{xz}^{0,i} \\ \gamma_{\theta z}^{0,i} \end{bmatrix} \tag{6c}$$

where $\bar{\kappa}$ is shear correction factor, and $\bar{\kappa}$=5/6 is assumed in this paper. A_{ij}, B_{ij} and D_{ij} are three kinds of stiffness, and they are obtained by Eq. (7)

$$(A_{ij}, B_{ij}, D_{ij}) = \int_{-h/2}^{h/2} Q_{ij}(z)(1, z, z^2)dz \tag{7}$$

The strain energy (UV) of the i th segment is displayed in Eq. (8)

$$U_\xi^i = \frac{1}{2}\iiint_V \begin{pmatrix} N_x^i\varepsilon_x^{0,i} + N_\theta^i\varepsilon_\theta^{0,i} \\ +N_{x\theta}^i\gamma_{x\theta}^{0,i} + M_x^i k_x^i \\ +M_\theta^i k_\theta^i + M_{x\theta}^i k_{x\theta}^i \\ +Q_x^i\gamma_{xz}^{0,i} + Q_\theta^i\gamma_{\theta z}^{0,i} \end{pmatrix} ABdxd\theta dz \tag{8}$$

In the equations above, A and B are namely Lamé parameters (Wang *et al*. 2017b, Guo *et al*. 2018). Then, the expression of strain energy can be expressed as $U^i = U_S^i + U_B^i + U_{BC}^i$, in which U_S^i, U_B^i and U_{BC}^i respectively represent the energy expressions of Stretching, Bending and Bending–Stretching coupling.

$$U_S^i = \frac{1}{2}\int\int\int \left\{ \begin{array}{l} A_{11}\left(\frac{1}{A}\frac{\partial u^i}{\partial x} + \frac{v^i}{AB}\frac{\partial A}{\partial \theta}\right)^2 \\ +A_{22}\left(\frac{1}{B}\frac{\partial v^i}{\partial \theta} + \frac{u^i}{AB}\frac{\partial B}{\partial x} + \frac{w^i}{R_\theta}\right)^2 \\ +A_{66}\left(\frac{A}{B}\frac{\partial}{\partial \theta}\left(\frac{u^i}{A}\right) + \frac{B}{A}\frac{\partial}{\partial x}\left(\frac{v^i}{B}\right)\right)^2 \\ +\bar{\kappa}A_{66}\left(\frac{1}{A}\frac{\partial w^i}{\partial x} + \psi_x^i\right)^2 \\ +2A_{12}\left(\frac{1}{A}\frac{\partial u^i}{\partial x} + \frac{v^i}{AB}\frac{\partial A}{\partial \theta}\right)\left(\frac{1}{B}\frac{\partial v^i}{\partial \theta} + \frac{u^i}{AB}\frac{\partial B}{\partial x} + \frac{w^i}{R}\right) \\ +\bar{\kappa}A_{66}\left(\frac{1}{B}\frac{\partial w^i}{\partial \theta} - \frac{v^i}{R} + \psi_\theta^i\right)^2 \end{array} \right\} ABdxd\theta dz \tag{9}$$

$$U_B^i = \frac{1}{2}\int\int\int \left\{ \begin{array}{l} D_{11}\left(\frac{1}{A}\frac{\partial \psi_x^i}{\partial x} + \frac{\psi_\theta^i}{AB}\frac{\partial A}{\partial \theta}\right)^2 \\ +D_{22}\left(\frac{1}{B}\frac{\partial \psi_\theta^i}{\partial \theta} + \frac{\psi_x^i}{AB}\frac{\partial B}{\partial x}\right)^2 \\ +D_{66}\left(\frac{A}{B}\frac{\partial}{\partial \theta}\left(\frac{\psi_x^i}{A}\right) + \frac{B}{A}\frac{\partial}{\partial x}\left(\frac{\psi_\theta^i}{B}\right)\right)^2 \\ +2D_{12}\left(\frac{1}{A}\frac{\partial \psi_x^i}{\partial x} + \frac{\psi_\theta^i}{AB}\frac{\partial A}{\partial \theta}\right)\left(\frac{1}{B}\frac{\partial \psi_\theta^i}{\partial \theta} + \frac{\psi_x^i}{AB}\frac{\partial B}{\partial x}\right) \end{array} \right\} ABdxd\theta dz \tag{10}$$

$$U_{BS}^i = \int\int\int \left\{ \begin{array}{l} B_{11}\left(\frac{1}{A}\frac{\partial u^i}{\partial x} + \frac{v^i}{AB}\frac{\partial A}{\partial \theta}\right)\left(\frac{1}{A}\frac{\partial \psi_x^i}{\partial x} + \frac{\psi_\theta^i}{AB}\frac{\partial A}{\partial \theta}\right) \\ +B_{12}\left(\frac{1}{A}\frac{\partial u^i}{\partial x} + \frac{v^i}{AB}\frac{\partial A}{\partial \theta}\right)\left(\frac{1}{B}\frac{\partial \psi_\theta^i}{\partial \theta} + \frac{\psi_x^i}{AB}\frac{\partial B}{\partial x}\right) \\ +B_{12}\left(\frac{1}{B}\frac{\partial v^i}{\partial \theta} + \frac{u^i}{AB}\frac{\partial B}{\partial x} + \frac{w^i}{R}\right)\left(\frac{1}{A}\frac{\partial \psi_x^i}{\partial x} + \frac{\psi_\theta^i}{AB}\frac{\partial A}{\partial \theta}\right) + \\ B_{66}\left(\frac{1}{A}\frac{\partial u^i}{\partial x} + \frac{v^i}{AB}\frac{\partial A}{\partial \theta}\right)\left(\frac{A}{B}\frac{\partial}{\partial \theta}\left(\frac{\psi_x^i}{A}\right) + \frac{B}{A}\frac{\partial}{\partial x}\left(\frac{\psi_\theta^i}{B}\right)\right) \\ +B_{22}\left(\frac{1}{B}\frac{\partial v^i}{\partial \theta} + \frac{u^i}{AB}\frac{\partial B}{\partial x} + \frac{w^i}{R}\right)\left(\frac{1}{B}\frac{\partial \psi_\theta^i}{\partial \theta} + \frac{\psi_x^i}{AB}\frac{\partial B}{\partial x}\right) \end{array} \right\} ABdxd\theta dz \tag{11}$$

The corresponding kinetic energy function of i th segment can be expressed as

$$\begin{aligned} T_\xi^i &= \frac{1}{2}\iiint_V \rho(z)\begin{bmatrix} \left(\dot{\bar{U}}^i\right)^2 + \left(\dot{\bar{V}}^i\right)^2 \\ +\left(\dot{\bar{W}}^i\right)^2 \end{bmatrix}\left(1 + \frac{z}{R}\right) ABdxd\theta dz \\ &= \frac{1}{2}\int_{x_0}^{x_1}\int_0^{2\pi} \Big\{ I_0[(\dot{u}^i)^2 + (\dot{v}^i)^2 + (\dot{w}^i)^2] \\ &\quad +2I_1\left(\dot{u}^i\dot{\psi}_x^i + \dot{v}^i\dot{\psi}_\theta^i\right) \\ &\quad +I_2\left[\left(\dot{\psi}_x^i\right)^2 + \left(\dot{\psi}_\theta^i\right)^2\right]\Big\} ABdxd\theta \end{aligned} \tag{12}$$

where the dot in Eq. (12) represent the differentiation about time, and

$$(I_0, I_1, I_2) = \int_{-h/2}^{h/2} \rho(z)\left(1+\frac{z}{R}\right)(1, z, z^2)\, dz \tag{13}$$

The energy stored in the end of boundary springs can be expressed as

$$\begin{aligned} U_b = &\frac{1}{2}\int_0^{2\pi}\int_{-h/2}^{h/2}\begin{Bmatrix} k_{u,0}u^2 + k_{v,0}v^2 + k_{w,0}w^2 \\ +k_{x,0}\psi_x^2 + k_{\theta,0}\psi_\theta^2 \end{Bmatrix}_{x=x_{l,0}} Bd\theta dz \\ &+\frac{1}{2}\int_0^{2\pi}\int_{-h/2}^{h/2}\begin{Bmatrix} k_{u,1}u^2 + k_{v,1}v^2 + k_{w,1}w^2 \\ +k_{x,1}\psi_x^2 + k_{\theta,1}\psi_\theta^2 \end{Bmatrix}_{x=x_{l,1}} Bd\theta dz \end{aligned} \tag{14}$$

where $k_{t,0}$ $(t = u, v, w, x, \theta)$ and $k_{t,1}$ respectively represent the spring values at two sides of FG circular cylindrical shell. For neighbor segments, the energy stored in connective springs can be expressed as

$$U_s^i = \frac{1}{2}\int_0^{2\pi}\int_{-\frac{h}{2}}^{\frac{h}{2}}\begin{Bmatrix} k_u(u^i - u^{i+1})^2 + k_v(v^i - v^{i+1})^2 \\ +k_w(w^i - w^{i+1})^2 \\ +k_x(\psi_x^i - \psi_x^{i+1})^2 + k_\theta\left(\psi_\theta^i - \psi_\theta^{i+1}\right)^2 \end{Bmatrix}_{i,i+1} Bd\theta dz \tag{15}$$

The total energy representing the boundary and connective conditions can be expressed in Eq. (16)

$$U_{BC} = U_b + \sum_{i=1}^{H-1} U_s^i \tag{16}$$

where H is the number of segments decomposed in FG circular cylindrical shell structure.

2.4 Admissible displacements and solution procedure

In present method, the displacement functions are handled by unified Jacobi polynomials along axial direction and Fourier series along circumferential direction. It is generally known that the recurrence relations of degree i in Jacobi polynomials $P_i^{(\alpha,\beta)}(\phi)$ (Bhrawy *et al*. 2015) are shown in Eq. (17)

$$P_0^{(\alpha,\beta)}(\phi) = 1 \tag{17a}$$

$$P_1^{(\alpha,\beta)}(\phi) = \frac{\alpha+\beta+2}{2}\phi - \frac{\alpha-\beta}{2} \tag{17b}$$

$$\begin{aligned} &P_i^{(\alpha,\beta)}(\phi) \\ &= \frac{\binom{\alpha+\beta}{+2i-1}\left\{\alpha^2 - \beta^2 + \phi\binom{\alpha+\beta}{+2i}\binom{\alpha+\beta}{+2i-2}\right\}}{2i(\alpha+\beta+i)(\alpha+\beta+2i-2)} P_{i-1}^{(\alpha,\beta)}(\phi) \\ &\quad - \frac{(\alpha+i-1)(\beta+i-1)(\alpha+\beta+2i)}{i(\alpha+\beta+i)(\alpha+\beta+2i-2)} P_{i-2}^{(\alpha,\beta)}(\phi) \end{aligned} \tag{17c}$$

where $\alpha, \beta > -1$ and $i = 2, 3, \ldots$

The displacement components of the shell segments can be written as

$$u = \sum_{m=0}^{M} U_m P_m^{(\alpha,\beta)}(\phi)\, cos(n\theta) e^{i\omega t} \tag{18a}$$

$$v = \sum_{m=0}^{M} V_m P_m^{(\alpha,\beta)}(\phi)\, sin(n\theta) e^{i\omega t} \tag{18b}$$

$$w = \sum_{m=0}^{M} W_m P_m^{(\alpha,\beta)}(\phi)\, cos(n\theta) e^{i\omega t} \tag{18c}$$

$$\psi_x = \sum_{m=0}^{M} \psi_{xm} P_m^{(\alpha,\beta)}(\phi)\, cos(n\theta) e^{i\omega t} \tag{18d}$$

$$\psi_\theta = \sum_{m=0}^{M} \psi_{\theta m} P_m^{(\alpha,\beta)}(\phi)\, cos(n\theta) e^{i\omega t} \tag{18e}$$

where U_m, V_m, W_m, ψ_{xm} and $\psi_{\theta m}$ are unknown coefficients. $P_m^{(\alpha,\beta)}(\phi)$ is the Jacobi polynomials of degree m for the displacement in axial direction. t is time. n and m represent the wave number in axial and circumferential directions, respectively. The highest degree of m is represented by M. The total Lagrangian energy functions L of FG circular cylindrical shell can be expressed in Eq. (19)

$$L = \sum_{i=1}^{H}(T^i - U^i) - U_{BC} \tag{19}$$

The differentiation with respect to unknown coefficients about Eq. (19) is shown in Eq. (20)

$$\frac{\partial L}{\partial \vartheta} = 0 \qquad \vartheta = U_m,\ V_m,\ W_m, \psi_{xm}, \psi_{\theta m} \tag{20}$$

By substituting Eqs. (8), (12), (16), (18) and Eq. (19) into Eq. (20), the form of Eq. (21) can be obtained

$$(K - \omega^2 M)B = 0 \tag{21}$$

where **K**, **M** and **B** respectively represent the stiffness matrix, mass matrix and vector of undetermined coefficient of the shell. The detailed description of Eq. (21) is given in Appendix A.

3. Numerical results and discussion

In this section, some numerical discussions are presented to verify the reliability and accuracy of proposed method in solving the vibration characteristics of uniform and stepped FG circular cylindrical shell structures. To simplify the study, the boundary conditions are represented by its first symbol. F, C, SD, SS and Ei (i = 1, 2, 3) represent the free, clamped, shear diaphragm, shear support and elastic restraint, respectively. The material parameters are chosen as: E_m = 70 GPa, E_c = 168 GPa, ρ_m = 2707 kg/m^3, ρ_c = 5700 kg/m^3, $\nu_m = \nu_c = 0.3$, M = 8, α = 0, β = −0.5,

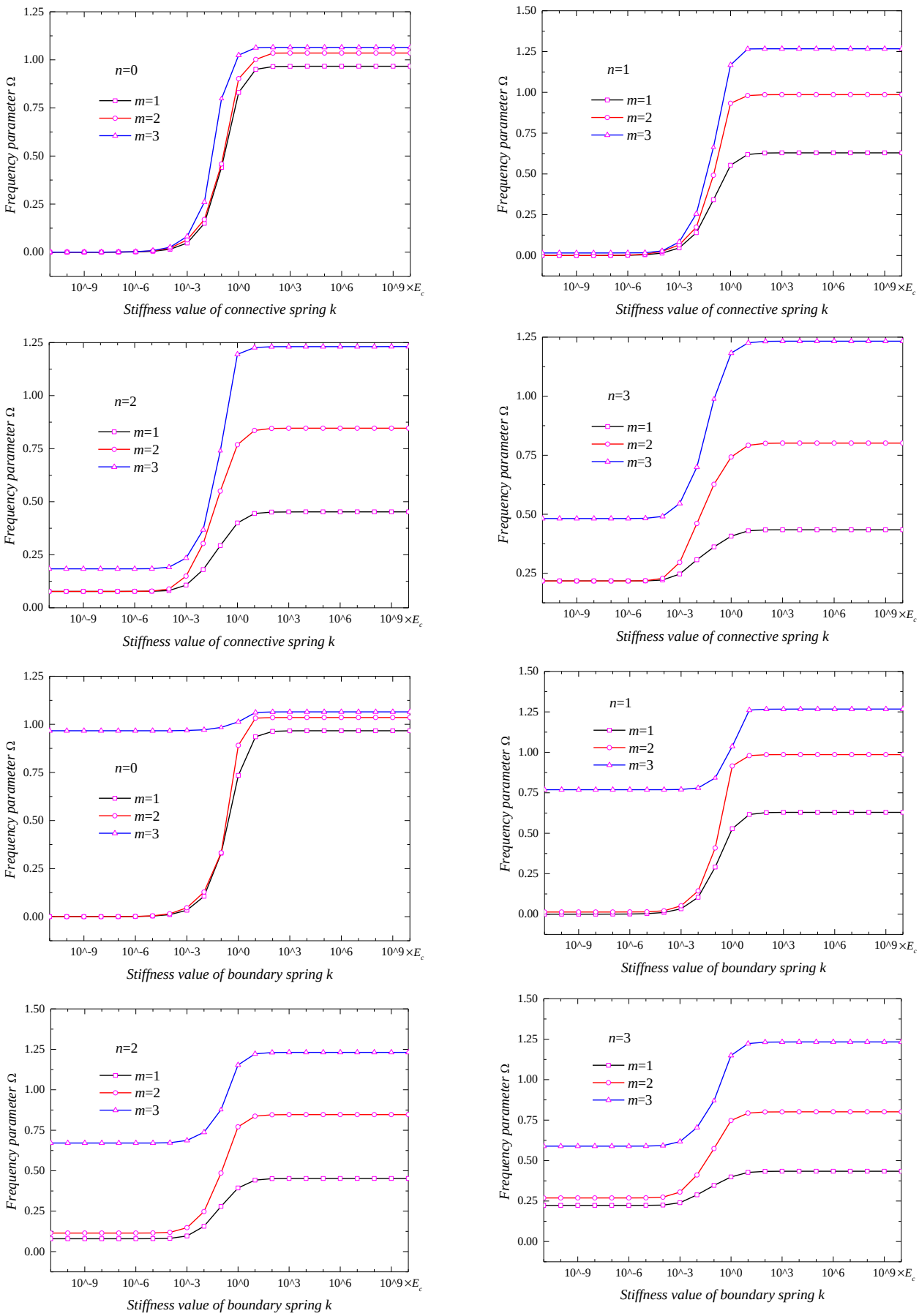

Fig. 3 Frequency parameters Ω of FG cylindrical shell with different boundary parameters

Table 1 The spring stiffness values of the general boundary conditions

BC	$k_{u,0}$, $k_{u,1}$	$k_{v,0}$, $k_{v,1}$	$k_{w,0}$, $k_{w,1}$	$k_{\varphi,0}$, $k_{\varphi,1}$	$k_{\theta,0}$, $k_{\theta,1}$
F	0	0	0	0	0
SD	0	10^3E_c	10^3E_c	0	0
SS	10^3E_c	10^3E_c	10^3E_c	0	10^3E_c
C	10^3E_c	10^3E_c	10^3E_c	10^3E_c	10^3E_c
E1	$10^{-3}E_c$	10^3E_c	10^3E_c	10^3E_c	10^3E_c
E2	10^3E_c	$10^{-3}E_c$	10^3E_c	10^3E_c	10^3E_c
E3	$10^{-3}E_c$	$10^{-3}E_c$	10^3E_c	10^3E_c	10^3E_c

H = 5. The geometrical dimensions of uniform and stepped FG circular cylindrical shell structures are chosen as follows: R = 1 m, L = 2 m. For uniform FG circular cylindrical shell, the thickness is selected as h = 0.1 m, and for the stepped FG circular cylindrical shell structure, the thickness is chosen as: $h_1 : h_2 : h_3 : h_4 = 0.1 : 0.15 : 0.2 : 0.25$. In addition, the results of this paper will dealt with the non-dimensional formulation: $\Omega = \omega R\sqrt{\frac{\rho_c}{E_c}}$.

3.1 Convergence study

Fig. 3 shows the frequency parameter Ω of uniform $\mathrm{FGM}_{\mathrm{I}(a=1/b=0.5/c=2/p=0.6)}$ cylindrical shell with various restraint parameters. For two kinds of springs, it can be seen clearly that the stiffness values in scope of 10^2E~$10^{10}E$ can guarantee the stable results. Thus, the general restraints of FG cylindrical shells can be obtained as Table 1 shown.

Fig. 4 displays the percentage error on the frequency parameters of uniform $\mathrm{FGM}_{\mathrm{I}(a=1/b=0.5/c=2/p=0.6)}$ cylindrical shell with different Jacobi parameters α and β. The results of frequency parameters $\alpha = \beta = 0$ are taken as the reference data. It can be see that different Jacobi parameter α and β have little change on the results of frequency parameters Ω, and the maximum percentage error does not exceed 2×10^{-6}. In other words, it implies that all of the polynomials can be used in present method. It is one of the most important discoveries of this paper.

Fig. 5 shows the frequency parameter Ω of uniform FG cylindrical shell with different truncation numbers. It is clearly see that stable convergence can be provided when the maximum degree M is no less than 5. To obtain more accurate results, the truncated number of the Jacobi polynomial is selected as M = 8 in this paper.

Fig. 6 shows the frequency parameter Ω of $\mathrm{FGM}_{\mathrm{I}(a=1/b=0.5/c=2/p=0.6)}$ cylindrical shell about the value of H. From Fig. 6, we can see clearly that the results converge quickly with the value of H increasing. However, when the number of segments reaches a certain level, increasing the number of segments will reduces the efficiency of the solution, and the accuracy of the solution is not greatly improved. We can also see that the accuracy of proposed

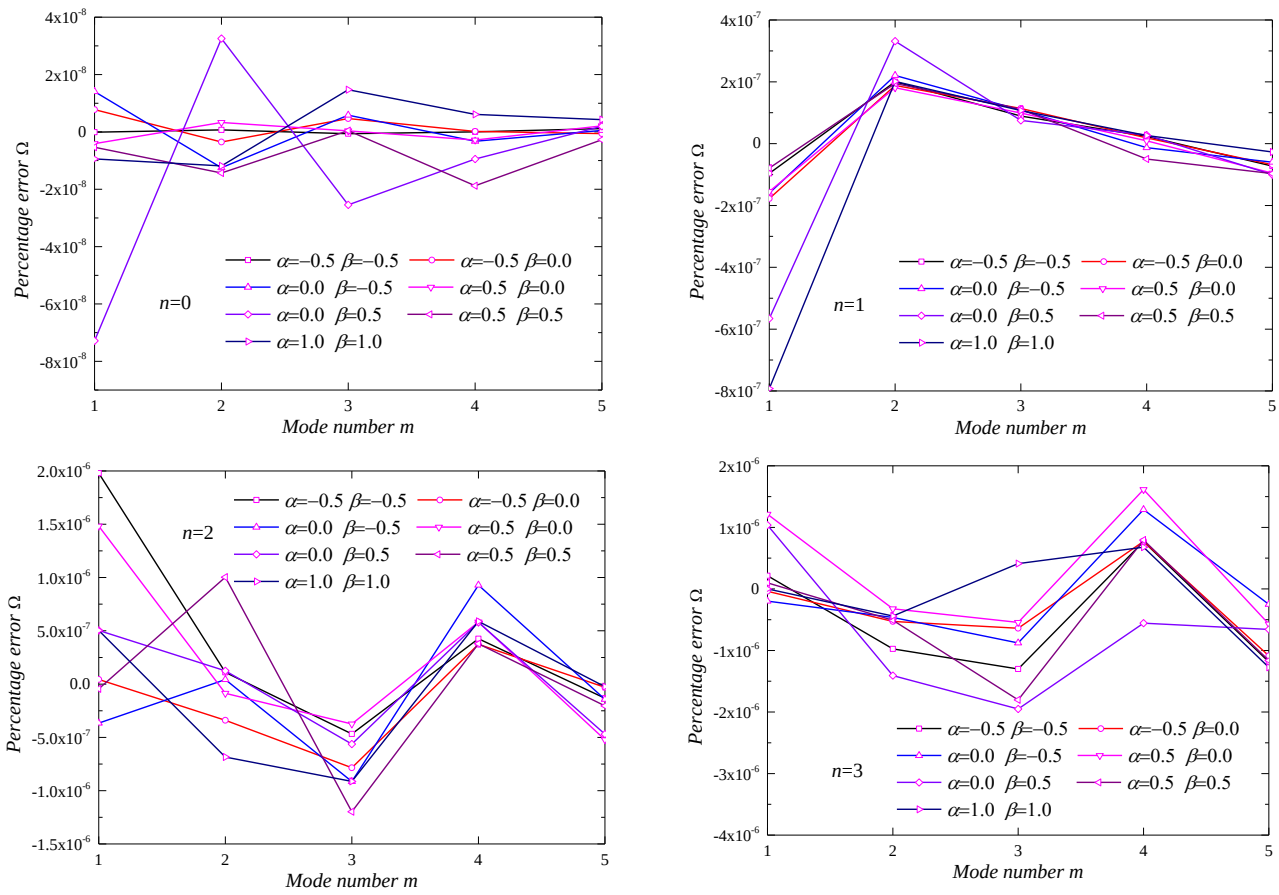

Fig. 4 Percentage error of frequency parameters Ω for α and β in FG cylindrical shell (BC: C–C)

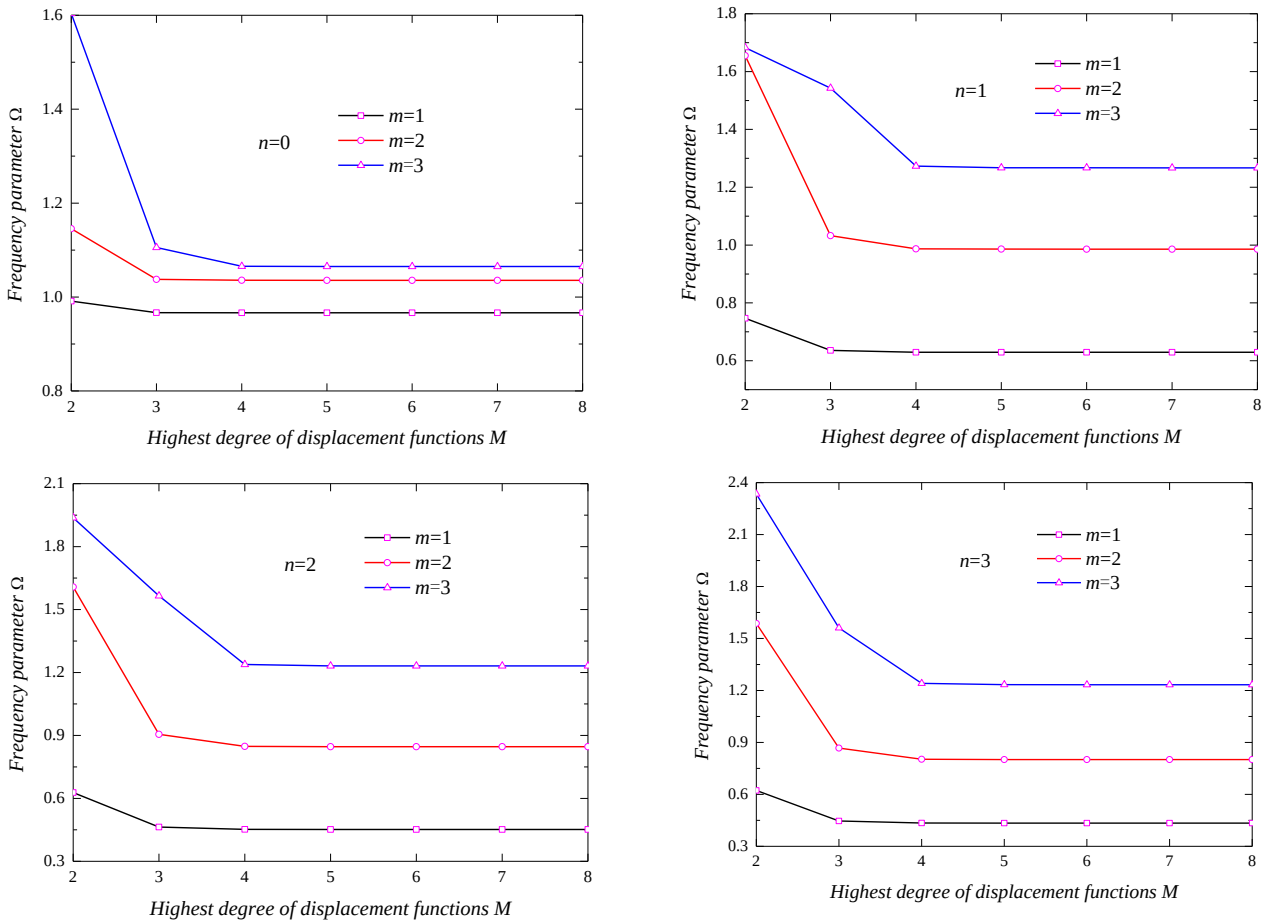

Fig. 5 Frequency parameters Ω for different truncation in FG cylindrical shell (BC: C–C)

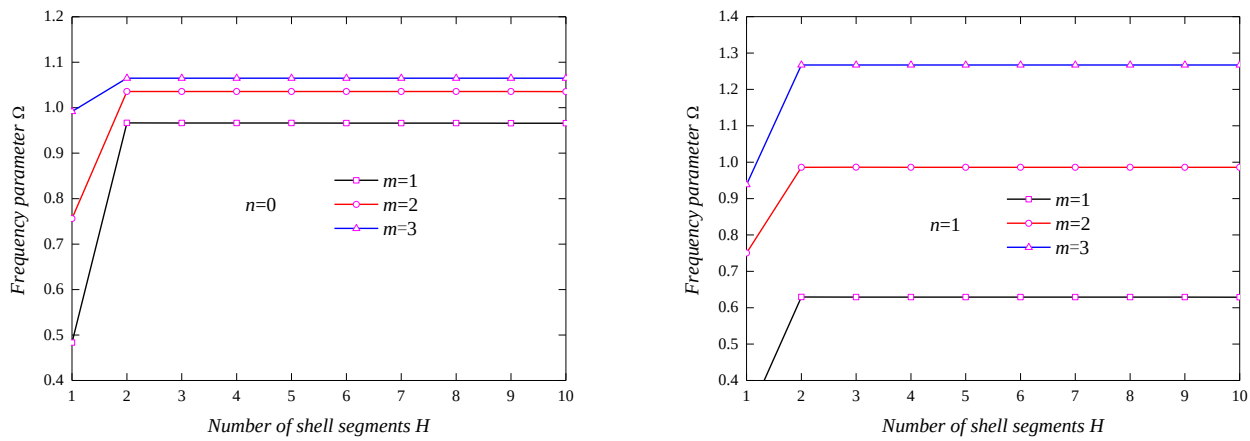

Fig. 6 Frequency parameters Ω for number of segments *H* in FG cylindrical shell (BC: C–C)

method can be guaranteed when *H* is higher than 2.

3.2 Free vibration behaviors of uniform FG cylindrical shell structure

Table 2 shows the accuracy of proposed method in solving free vibration characteristics of uniform FG cylindrical shell subject to classical boundary conditions, and all results are compared with those obtained by FEM. All the results obtained by FEM have converged to stable when the mesh size is chosen as 0.02 m. It should be noted that all finite element modeling in this paper is a special form of FG material. From Table 2, we can easily get that the proposed method has ability to investigate the vibration characteristics of uniform FG cylindrical shell subject to classical boundary conditions.

Table 3 also shows the accuracy of proposed method in solving the free vibration characteristics of uniform FG cylindrical shell structure, and all the results are compared with those obtained by published literatures. We can easily

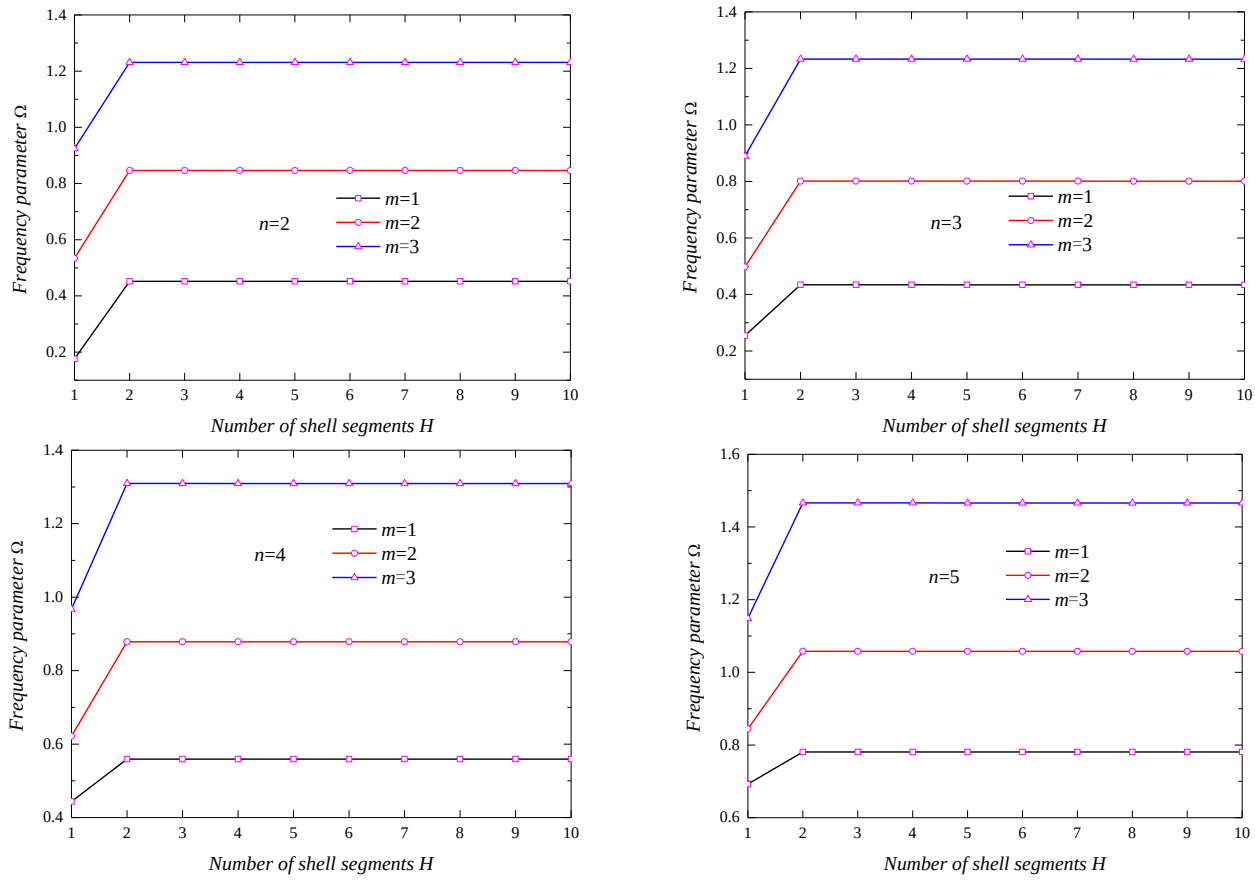

Fig. 6 Continued

Table 2 Comparison of frequency parameter $\Omega = \omega R\sqrt{\frac{\rho_c}{E_c}}$ for uniform $FGM_{I(a/b/c/p=0)}$ circular cylindrical shell

n	m	C–C		C–F		SD–SD	
		Present	FEM	Present	FEM	Present	FEM
1	1	0.6336	0.6338	0.2935	0.2936	0.6035	0.6036
	2	0.9924	0.9922	0.7555	0.7555	0.9335	0.9333
	3	1.2742	1.2747	0.9443	0.9451	1.1541	1.1541
2	1	0.4547	0.4539	0.1768	0.1753	0.3721	0.3707
	2	0.8513	0.8501	0.5370	0.5344	0.7752	0.7737
	3	1.2374	1.2369	0.9288	0.9267	1.1059	1.1048
3	1	0.4360	0.4344	0.2545	0.2529	0.3536	0.3510
	2	0.8047	0.8021	0.4990	0.4943	0.7095	0.7063
	3	1.2384	1.2365	0.8924	0.8882	1.0996	1.0970

get that the proposed method is very accurate in solving the vibration characteristics of FG cylindrical shell structure. Thus, from Tables 2−3, we can conclude that the proposed method has the ability to analyze the free vibration characteristics of FG cylindrical shell subjected to general boundary conditions. However, the boundary conditions of the structures are usually very complex in practical engineering applications. So the following content will be focused on the free vibration characteristics of FG cylindrical shell subject to complex boundary conditions.

Table 4 shows the numerical results for free vibration characteristics of uniform FG cylindrical shell with various restraints and power-law exponent p. From Table 4, it can be seen clearly that the vibration characteristics are not only affected by the boundary restraints, but also the power-law index p. In addition, the frequency parameter values will be lower when the power-law exponent p increasing under the same boundary restraint, regardless of the FGM_I and the

Table 3 Comparison of frequency (Hz) for uniform FGM circular cylindrical shell with classical restraints

p	BC	Method	n						
			1	2	3	4	5	6	7
			FGM_I (a=1/b=0.5/c=2/p)						
0.6	C–C	Present	543.68	390.51	375.21	483.25	674.80	921.28	1209.49
		Su (2014)	543.89	390.69	375.35	483.34	674.86	921.34	1209.54
		Qu (2013)	543.84	390.65	375.30	483.30	674.82	921.30	1209.50
	SD–SD	Present	517.60	319.25	304.27	437.72	645.96	901.31	1194.60
		Su (2014)	517.86	319.47	304.46	437.89	646.13	901.49	1194.79
		Qu (2013)	517.81	319.41	304.35	437.76	645.99	901.34	1194.63
	SS–SS	Present	528.06	363.68	346.81	461.35	658.79	909.20	1200.09
		Su (2014)	528.28	363.87	346.93	461.41	658.83	909.22	1200.10
		Qu (2013)	528.23	363.83	346.90	461.40	658.82	909.22	1200.10
5	C–C	Present	526.62	380.10	369.16	479.19	670.54	915.44	1200.98
		Su (2014)	526.75	380.22	369.25	479.25	670.59	915.48	1201.03
		Qu (2013)	526.72	380.18	369.21	479.22	670.55	915.45	1200.99
	SD–SD	Present	500.08	309.51	299.70	434.77	642.37	895.93	1186.47
		Su (2014)	500.27	309.70	299.88	434.94	642.54	896.10	1186.64
		Qu (2013)	500.21	309.62	299.76	434.80	642.40	895.95	1186.49
	SS–SS	Present	512.22	357.05	345.27	460.67	656.81	904.95	1192.76
		Su (2014)	512.35	357.16	345.35	460.71	656.84	904.97	1192.77
		Qu (2013)	512.32	357.14	345.33	460.70	656.83	904.96	1192.76
			FGM_{II} (a=1/b=0.5/c=2/p)						
0.6	C–C	Present	543.64	390.33	374.60	481.90	672.58	918.12	1,205.34
		Su (2014)	543.86	390.51	374.74	481.99	672.64	918.18	1,205.39
		Qu (2013)	543.81	390.47	374.69	481.94	672.60	918.14	1,205.36
	SD–SD	Present	517.77	319.55	304.01	436.49	643.77	898.15	1,190.44
		Su (2014)	518.02	319.75	304.17	436.65	643.94	898.33	1,190.62
		Qu (2013)	517.98	319.72	304.09	436.53	643.80	898.18	1,190.46
	SS–SS	Present	526.89	359.90	342.05	457.06	654.71	904.83	1,195.11
		Su (2014)	527.11	360.09	342.17	457.13	654.74	904.84	1,195.12
		Qu (2013)	527.06	360.05	342.14	457.11	654.73	904.84	1,195.11
5	C–C	Present	526.46	379.37	366.99	474.54	662.99	904.73	1,186.97
		Su (2014)	526.59	379.49	367.08	474.60	663.04	904.78	1,187.02
		Qu (2013)	526.56	379.45	367.04	474.57	663.00	904.74	1,186.98
	SD–SD	Present	500.63	310.40	298.67	430.55	634.95	885.23	1,172.40
		Su (2014)	500.80	310.51	298.78	430.67	635.09	885.39	1,172.57
		Qu (2013)	500.76	310.50	298.72	430.57	634.97	885.25	1,172.42
	SS–SS	Present	508.50	345.10	330.32	447.06	643.58	890.53	1,176.20
		Su (2014)	508.63	345.20	330.38	447.09	643.60	890.54	1,176.20
		Qu (2013)	508.60	345.18	330.37	447.08	643.59	890.54	1,176.20

FGM_{II}.

Tables 5-6 respectively represent the numerical results for vibration characteristics of uniform FG cylindrical shell with classical, elastic and classical–elastic restraints.

Various thicknesses of the structure are also considered. We can easily get that the thickness of FG cylindrical shell will mainly affect the results of frequency parameter, and the greater value of thickness is chosen, the higher requency will obtained. In addition, some mode shapes are demonstrated of FGM_I cylindrical shell in Table 5 with different boundary restraints in Figs. 7-9.

Table 4 Frequencies (Hz) of uniform FGM cylindrical shell with various restraints and power-law exponents p (h/R = 0.15, R = 1 m; m = 1)

p	Boundary conditions											
	SD–SD	C–C	C–SD	SS–SS	C–SS	SD–SS	E1–E1	E2–E2	E3–E3	E1–E2	E1–E3	E2–E3
FGM$_{\mathrm{I}}$ (a=1/b=0.5/c=2/p)												
0	525.04	563.49	537.24	535.20	548.45	525.26	536.30	332.11	296.77	388.00	312.28	326.09
0.5	521.70	560.30	534.00	532.76	545.67	522.06	533.14	330.49	295.30	385.96	310.74	324.49
1	518.48	557.25	530.90	530.38	542.98	519.00	530.16	328.89	293.88	383.97	309.24	322.91
2	512.83	551.94	525.49	526.02	538.18	513.67	524.99	326.10	291.41	380.51	306.61	320.16
5	503.10	542.75	516.09	517.20	529.16	504.22	515.50	321.88	287.27	374.88	302.44	315.99
10	498.15	537.49	510.97	510.99	523.38	498.96	509.90	319.68	284.96	371.82	300.18	313.83
20	495.43	533.77	507.81	506.80	519.41	495.93	506.78	317.21	283.15	369.16	298.07	311.42
50	493.47	530.59	505.34	503.74	516.31	493.78	504.78	314.38	281.46	366.48	295.84	308.66
FGM$_{\mathrm{II}}$ (a=1/b=0.5/c=2/p)												
0	525.04	563.49	537.24	535.20	548.45	525.26	536.30	332.11	296.77	388.00	312.28	326.09
0.5	522.02	560.25	534.15	531.29	544.83	522.17	533.14	330.47	295.29	385.97	310.73	324.47
1	519.07	557.16	531.18	527.71	541.45	519.22	530.16	328.84	293.87	383.99	309.21	322.88
2	513.79	551.78	525.95	521.68	535.68	514.01	524.99	326.02	291.40	380.56	306.59	320.11
5	504.33	542.51	516.68	511.71	525.97	504.64	515.50	321.78	287.28	374.98	302.42	315.95
10	499.10	537.29	511.43	506.76	520.92	499.29	509.90	319.61	284.97	371.91	300.17	313.80
20	496.00	533.64	508.08	504.27	517.94	496.13	506.78	317.17	283.16	369.22	298.07	311.40
50	493.71	530.53	505.46	502.63	515.66	493.86	504.78	314.36	281.47	366.50	295.84	308.66

Table 5 Frequencies (Hz) for uniform FGM cylindrical shell with classical and elastic boundaries (m = 1)

n	h/R	Boundary conditions											
		SD–SD	C–C	C–SD	SS–SS	C–SS	SD–SS	E1–E1	E2–E2	E3–E3	E1–E2	E1–E3	E2–E3
FGM$_{\mathrm{I}}$ (a=1/b=0.5/c=2/p)													
1	0.05	498.30	514.20	501.31	508.77	511.44	498.75	503.91	244.81	241.33	319.16	241.72	241.34
	0.1	500.08	526.62	507.67	512.22	519.16	500.83	515.41	290.14	271.42	350.67	278.90	285.21
	0.15	503.10	542.75	516.09	517.20	529.16	504.22	515.50	321.88	287.27	374.88	302.44	315.99
2	0.05	291.00	344.89	315.51	335.79	340.25	310.94	303.00	268.39	249.23	269.93	267.82	256.35
	0.1	309.51	380.10	341.85	357.05	368.01	330.67	340.31	324.71	304.04	321.38	317.68	311.84
	0.15	336.48	424.96	376.77	387.00	404.66	358.93	387.00	378.45	358.14	373.27	369.27	365.71
3	0.05	210.49	273.12	241.35	262.39	267.57	236.42	228.41	254.74	223.18	240.71	225.56	238.77
	0.1	299.70	369.16	332.42	345.27	356.44	322.00	335.41	358.67	333.48	346.38	334.39	345.69
	0.15	398.83	476.29	434.32	442.33	457.99	419.85	447.79	468.33	446.69	457.41	447.21	457.05
FGM$_{\mathrm{II}}$ (a=1/b=0.5/c=2/p)													
1	0.05	498.43	514.12	501.36	506.84	510.40	498.75	503.90	244.79	241.33	319.20	241.72	241.33
	0.1	500.63	526.46	507.91	508.50	517.06	500.98	515.39	290.09	271.42	350.74	278.89	285.19
	0.15	504.33	542.51	516.68	511.71	525.97	504.64	515.50	321.78	287.28	374.98	302.42	315.95
2	0.05	291.21	344.65	315.49	329.37	336.85	308.18	302.82	268.17	249.04	269.74	267.63	256.14
	0.1	310.40	379.37	341.94	345.10	361.42	325.72	339.70	323.97	303.38	320.72	317.04	311.16
	0.15	338.09	423.43	376.87	370.07	394.97	352.09	385.66	376.88	356.70	371.84	367.87	364.23
3	0.05	210.43	272.62	241.09	253.40	262.65	232.00	227.90	254.22	222.67	240.20	225.06	238.26
	0.1	298.67	366.99	330.95	330.32	347.36	314.28	333.23	356.46	331.28	344.19	332.19	343.49
	0.15	395.74	471.49	430.63	422.46	444.90	408.80	443.03	463.47	441.90	452.61	442.44	452.24

Table 6 Frequencies (Hz) for uniform FGM cylindrical shell with classical-elastic restraints (m=1)

n	h/R	Boundary conditions											
		C–E1	C–E2	C–E3	SD–E1	SD–E2	SD–E3	SS–E1	SS–E2	SS–E3	F–E1	F–E2	F–E3
							FGM$_{\mathrm{I}}$ (a=1/b=0.5/c=2/p)						
1	0.05	504.10	358.05	352.52	501.07	317.69	240.42	501.48	356.70	351.26	20.92	156.10	18.66
	0.1	515.41	390.12	387.14	507.48	346.60	276.28	508.09	386.33	383.60	30.14	177.37	25.92
	0.15	530.26	415.53	413.54	514.49	367.15	298.15	516.85	408.20	406.63	38.74	190.27	33.29
2	0.05	321.55	299.84	294.75	296.90	265.31	262.99	316.79	296.65	291.24	45.71	122.91	43.66
	0.1	357.73	348.79	341.25	324.31	308.16	303.89	345.38	339.30	330.92	86.82	145.97	84.56
	0.15	403.40	399.15	390.95	360.24	350.06	345.23	382.76	382.08	372.66	126.44	173.91	124.23
3	0.05	250.71	263.11	247.95	219.22	232.20	216.77	245.37	258.30	242.96	105.93	124.42	105.20
	0.1	351.97	363.64	351.05	316.44	327.84	315.77	339.71	351.78	339.08	207.59	218.07	206.97
	0.15	461.65	472.15	461.17	421.26	431.08	420.96	443.91	454.66	443.66	304.08	311.92	303.53
							FGM$_{\mathrm{II}}$ (a=1/b=0.5/c=2/p)						
1	0.05	504.09	358.03	352.48	501.13	317.75	240.42	501.43	354.96	348.90	20.92	156.09	18.67
	0.1	515.39	390.07	387.06	507.76	346.77	276.27	508.02	383.02	379.46	30.15	177.35	25.94
	0.15	530.25	415.44	413.40	514.58	367.52	298.13	516.83	403.21	400.60	38.77	190.23	33.32
2	0.05	321.34	299.60	294.54	296.93	265.23	262.93	313.80	293.32	288.03	45.50	122.77	43.45
	0.1	357.08	348.06	340.57	324.51	308.05	303.87	339.59	332.65	324.70	85.99	145.35	83.72
	0.15	401.99	397.60	389.48	360.57	349.84	345.18	374.26	372.16	363.52	124.62	172.39	122.40
3	0.05	250.21	262.60	247.44	218.95	231.90	216.49	240.56	253.63	238.24	105.25	123.82	104.52
	0.1	349.80	361.45	348.87	314.94	326.29	314.24	330.85	342.86	330.26	205.00	215.56	204.38
	0.15	456.88	467.32	456.39	417.56	427.29	417.23	431.17	441.68	430.92	298.62	306.51	298.07

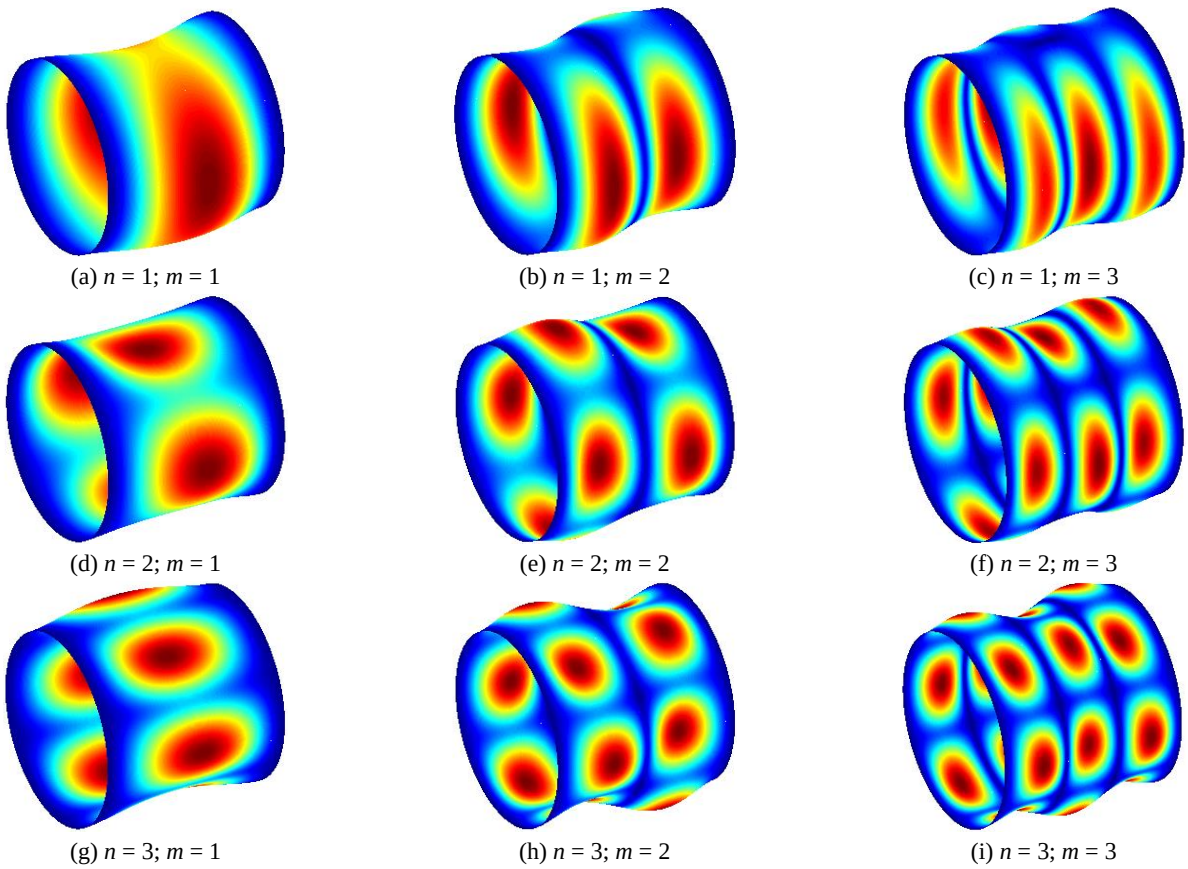

(a) n = 1; m = 1 (b) n = 1; m = 2 (c) n = 1; m = 3

(d) n = 2; m = 1 (e) n = 2; m = 2 (f) n = 2; m = 3

(g) n = 3; m = 1 (h) n = 3; m = 2 (i) n = 3; m = 3

Fig. 7 Mode shapes of uniform FG circular cylindrical shell (BC: C–C)

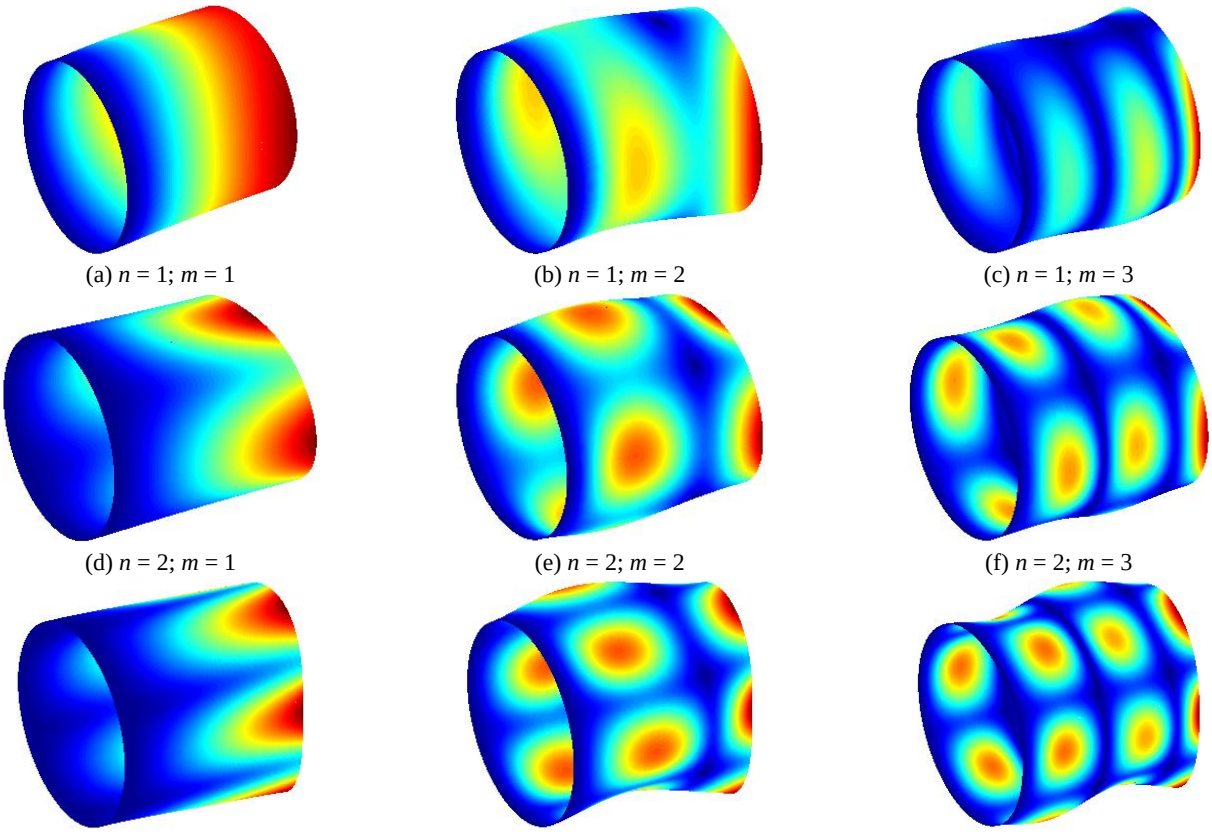

(a) $n = 1$; $m = 1$ (b) $n = 1$; $m = 2$ (c) $n = 1$; $m = 3$

(d) $n = 2$; $m = 1$ (e) $n = 2$; $m = 2$ (f) $n = 2$; $m = 3$

(g) $n = 3$; $m = 1$ (h) $n = 3$; $m = 2$ (i) $n = 3$; $m = 3$

Fig. 8 Mode shapes of uniform FG circular cylindrical shell (BC: C–F)

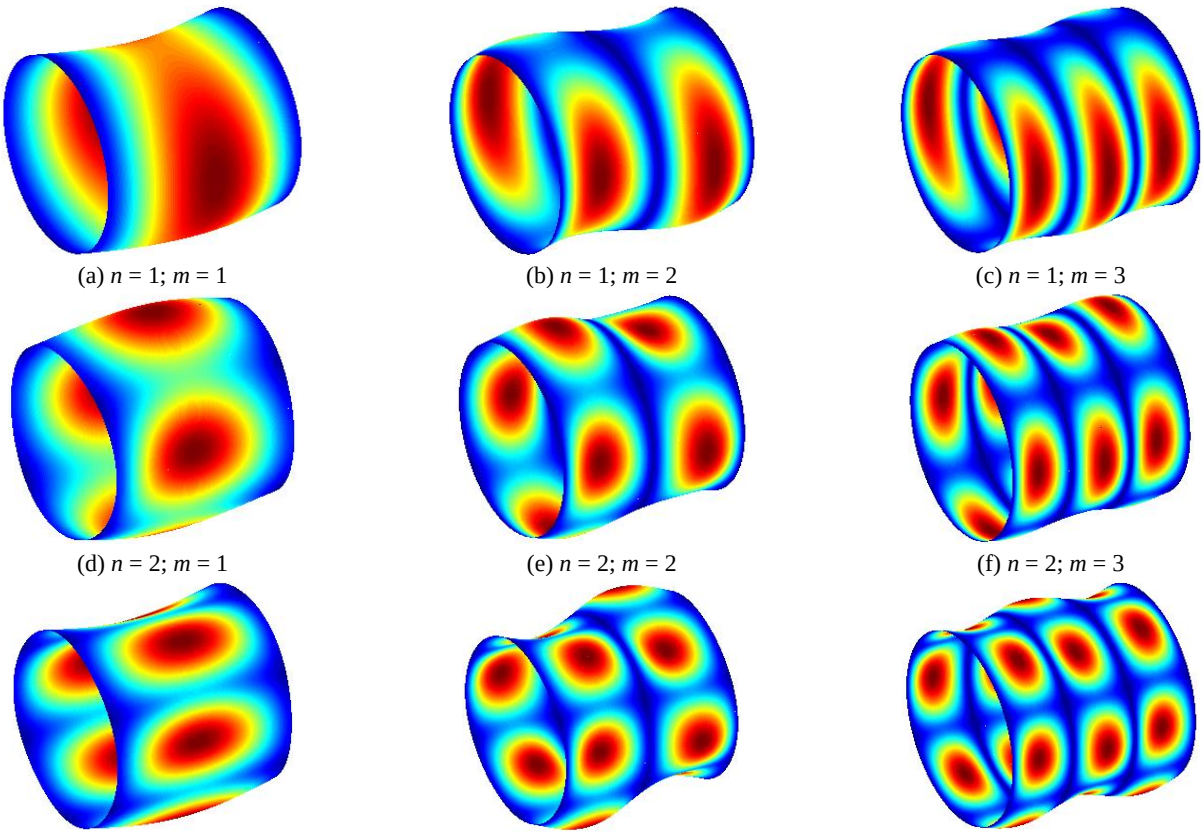

(a) $n = 1$; $m = 1$ (b) $n = 1$; $m = 2$ (c) $n = 1$; $m = 3$

(d) $n = 2$; $m = 1$ (e) $n = 2$; $m = 2$ (f) $n = 2$; $m = 3$

(g) $n = 3$; $m = 1$ (h) $n = 3$; $m = 2$ (i) $n = 3$; $m = 3$

Fig. 9 Mode shapes of uniform FG circular cylindrical shell (BC: SD–SD)

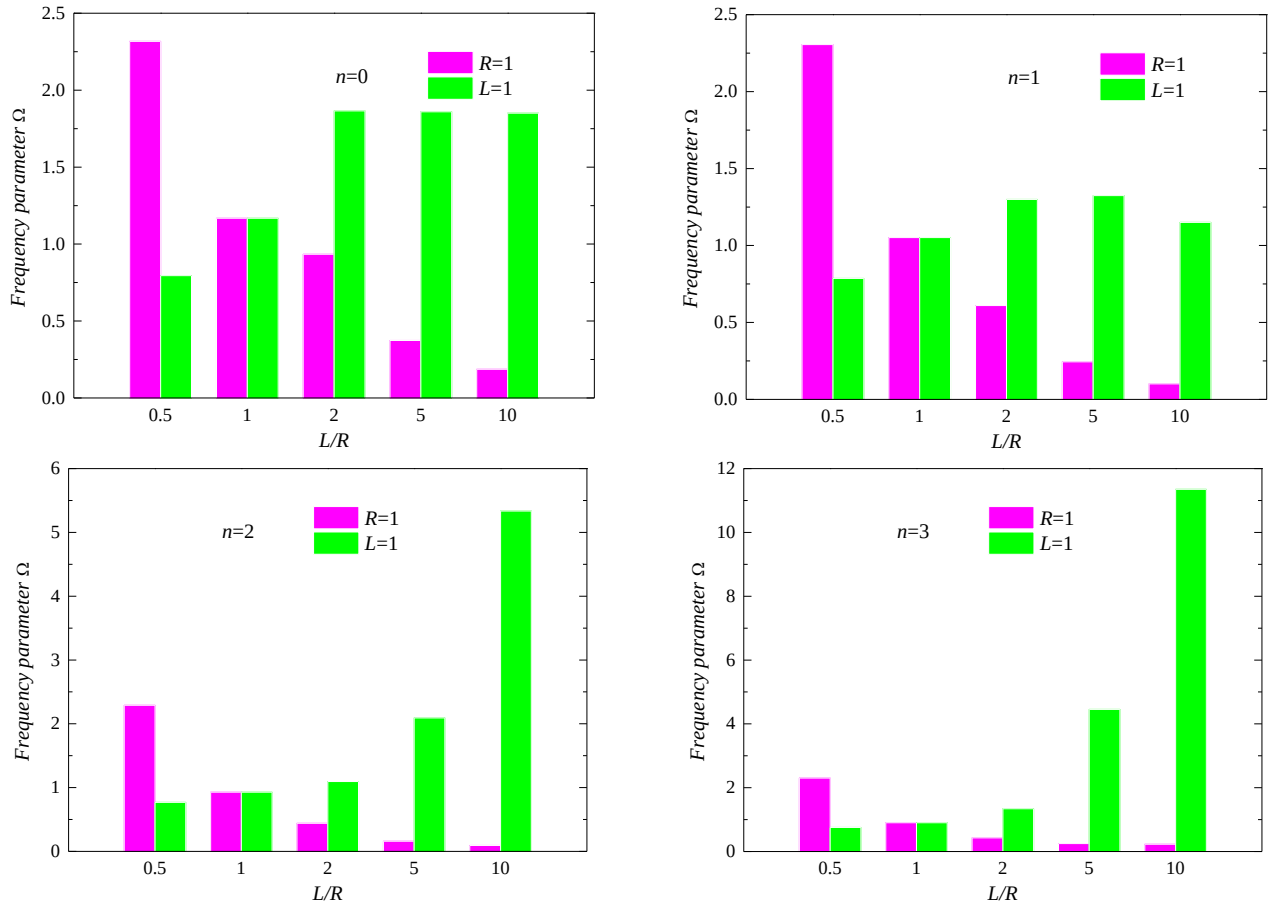

Fig. 10 Frequency parameters Ω for different dimensions in uniform FG circular cylindrical shell (BC: C–C)

Table 7 Comparison of frequency parameter $\Omega = \omega R\sqrt{\frac{\rho_c}{E_c}}$ for stepped $FGM_{I(a/b/c/p=0)}$ circular cylindrical shell

n	m	C–C		C–F		SD–SD	
		Present	FEM	Present	FEM	Present	FEM
1	1	0.6521	0.6519	0.3776	0.3769	0.5075	0.5068
	2	1.1102	1.1097	0.8401	0.8390	0.6929	0.6960
	3	1.5221	1.5225	1.1435	1.1490	0.9972	1.0002
2	1	0.5202	0.5169	0.2515	0.2504	0.4008	0.3991
	2	1.0165	1.0141	0.6605	0.6571	0.8906	0.8862
	3	1.5572	1.5548	1.1085	1.1043	1.3667	1.3725
3	1	0.5934	0.5917	0.3401	0.3388	0.5065	0.5046
	2	1.0572	1.0534	0.6916	0.6904	0.9240	0.9194
	3	1.6361	1.6310	1.1555	1.1511	1.4518	1.4484

Fig. 10 shows the frequency parameter Ω of $FGM_{I(a=1/b=0.5/c=2/p=5)}$ cylindrical shell with various scale ratios. We can see that the results are mainly affected by the geometric dimensions L and R, and the value of L and R is obviously different when the ratio of L/R is chosen as the different value.

3.3 Free vibration behaviors of stepped FG cylindrical shell structure

Table 7 shows the accuracy of presented method in solving free vibration characteristics of stepped FG cylindrical shell subject to classical boundary conditions, and all the results are compared with those obtained by FEM. The geometrical and material parameters of FEM are

Table 8 Comparison of frequencies (Hz) for two stepped circular cylindrical shell (L/R = 10, R = 1 m, h_1:h_2 = 0.01:0.005, h_1 = 0.01; m = 1)

n	SD–SD		C–F		C–SD		C–C	
	Present	Tang (2017)	Present	Tang (2017)	Present	Tang (2017)	Present	Tang (2017)
1	307.53	307.52	160.49	160.26	449.03	448.39	532.45	531.19
2	112.87	112.82	59.22	59.09	174.36	174.03	225.75	224.95
3	111.77	111.68	70.31	70.19	124.40	124.24	151.21	150.83
4	158.55	158.44	118.57	118.40	158.56	158.45	183.75	183.39
5	207.75	207.69	186.70	186.46	207.76	207.70	225.24	224.96
6	282.80	282.80	272.15	271.84	282.80	282.80	291.64	291.52
7	380.06	380.11	373.78	373.41	380.06	380.11	384.41	384.41
8	495.73	495.86	491.25	490.83	495.73	495.86	498.02	498.11

Table 9 Frequencies (Hz) of stepped FGM cylindrical shell with various boundaries and power-law exponents p (h/R = 0.1:0.15:0.2:0.25, R = 1 m; m = 1)

p	Boundary conditions										
	SD–SD	C–C	C–SD	SS–SS	C–SS	SD–SS	E1–E1	E2–E2	E3–E3	E1–E2	E1–E3
					FGM_{I} (a=1/b=0.5/c=2/p)						
0	438.50	563.93	484.94	528.58	535.78	528.22	457.51	348.03	251.28	419.66	376.05
0.5	435.75	560.72	481.86	526.53	533.72	525.98	455.11	346.48	251.02	417.60	374.56
1	433.12	557.64	478.93	524.47	531.62	523.72	452.82	344.95	250.70	415.59	373.11
2	428.49	552.30	473.83	520.55	527.62	519.46	448.83	342.32	250.14	412.08	370.59
5	420.33	543.19	465.04	512.09	519.21	510.73	441.83	338.52	249.61	406.45	366.47
10	415.99	538.08	460.43	505.67	512.95	504.61	437.89	336.69	249.45	403.40	364.18
20	413.61	534.34	457.77	501.12	508.34	500.41	435.37	334.46	248.59	400.56	362.20
50	411.97	531.05	455.80	497.72	504.72	497.23	433.39	331.77	247.26	397.60	360.21
					FGM_{II} (a=1/b=0.5/c=2/p)						
0	438.50	563.93	484.94	528.58	535.78	528.22	457.51	348.03	251.28	419.66	376.05
0.5	435.89	560.74	482.21	524.30	531.51	524.08	455.14	346.61	250.94	417.54	374.51
1	433.39	557.67	479.59	520.41	527.60	520.26	452.89	345.20	250.58	415.48	373.01
2	428.97	552.33	474.95	513.97	521.10	513.84	448.99	342.72	249.96	411.92	370.42
5	421.06	543.19	466.57	503.78	510.98	503.63	442.14	339.03	249.44	406.27	366.23
10	416.60	538.06	461.66	499.31	506.64	499.19	438.17	337.08	249.35	403.26	363.98
20	413.99	534.33	458.52	497.31	504.56	497.16	435.55	334.69	248.53	400.48	362.08
50	412.14	531.05	456.13	496.04	503.06	495.81	433.47	331.87	247.24	397.57	360.15

the same as Table 2 except the thickness distribution. From Table 7, we can get that the present method has ability to investigate the vibration characteristics of stepped FG cylindrical shell subject to classical boundary conditions.

Table 8 shows the frequency parameters Ω of stepped FG cylindrical shell with different thickness distribution, and the results in Table 8 are contrasted with the single and isotropic two stepped cylindrical shell due to the lack of the reference data. We can see clearly that the results in Table 8 closely agree with the published literature for dealing with the stepped cylindrical shell. And from Tables 7-8, we can conclude that proposed method also has the ability to study the vibration characteristics of stepped FG cylindrical shell structure. Tables 9-10 show the numerical results for free vibration characteristics of stepped FG cylindrical shell with classical, elastic and classical–elastic restraints, respectively. The phenomenon of the results is as same as Tables 5-6.

4. Conclusions

The paper presents a unified Jacobi–Ritz formulation to analyze the free vibration characteristics of uniform and stepped FG circular cylindrical shell structures subject to complex boundary conditions. The multi-segment partitioning strategy and first-order shear deformation theory were used to establish analytical model. The

Table 10 Frequencies (Hz) of stepped FGM cylindrical shell with classical-elastic restraints and various power-law exponents p (h/R = 0.15, R = 1 m; m = 1)

p	Boundary conditions											
	C–E1	C–E2	C–E3	SD–E1	SD–E2	SD–E3	SS–E1	SS–E2	SS–E3	F–E1	F–E2	F–E3
FGM$_{\mathrm{I}}$ (a=1/b=0.5/c=2/p)												
0	507.92	434.19	433.95	452.83	415.34	373.82	502.94	428.55	428.36	72.97	265.34	63.54
0.5	505.07	432.00	431.76	450.27	413.23	372.14	499.68	426.66	426.42	73.25	263.77	64.08
1	502.34	429.87	429.62	447.80	411.17	370.52	496.62	424.78	424.49	73.47	262.27	64.54
2	497.57	426.16	425.89	443.46	407.56	367.69	491.37	421.40	421.05	73.86	259.73	65.34
5	489.35	420.18	419.88	435.92	401.71	363.00	482.71	415.54	415.11	75.04	255.78	67.16
10	484.78	416.93	416.61	431.94	398.59	360.37	478.39	411.94	411.52	75.94	253.89	68.39
20	481.62	413.97	413.64	429.55	395.87	358.23	475.79	408.73	408.37	75.93	252.36	68.62
50	478.93	410.90	410.59	427.72	393.11	356.16	473.69	405.59	405.30	75.39	250.82	68.31
FGM$_{\mathrm{II}}$ (a=1/b=0.5/c=2/p)												
0	507.92	434.19	433.95	452.83	415.34	373.82	502.94	428.55	428.36	72.97	265.34	63.54
0.5	505.10	431.96	431.72	450.34	413.19	372.09	500.47	426.01	425.85	73.37	264.18	64.18
1	502.40	429.79	429.54	447.94	411.09	370.43	498.07	423.59	423.45	73.70	263.01	64.73
2	497.71	426.02	425.77	443.73	407.44	367.53	493.77	419.48	419.37	74.25	260.93	65.66
5	489.65	420.02	419.75	436.37	401.58	362.77	485.85	413.13	413.03	75.57	257.32	67.61
10	485.05	416.81	416.51	432.33	398.50	360.18	480.85	410.09	409.95	76.37	255.07	68.75
20	481.79	413.89	413.59	429.80	395.82	358.11	477.27	407.63	407.44	76.19	253.07	68.84
50	479.01	410.87	410.57	427.83	393.09	356.11	474.34	405.11	404.89	75.51	251.12	68.41

displacement functions are handled by the Jacobi polynomials along the axial direction and Fourier series along the circumferential direction. Based on the penalty method and Rayleigh–Ritz method, the free vibration characteristics of FG cylindrical shells are analyzed. The most important discovery of this paper is the unified Jacobi polynomials, which makes the permissible functions very easy to select in contrast with other approaches. In addition, to test the convergence, the effect of boundary penalty parameters, number of shell segments, Jacobi parameters and the maximum degree of the permissible displacement functions on free vibration characteristics of FG cylindrical shell are examined. The stability and accuracy of presented approach have been verified by comparing with the results of FEM and published literatures. The results of this paper may be used as the reference data in future for related researches.

Acknowledgments

Funding: This study was funded by National Natural Science Foundation of China (51209052, 51709063), National key Research and Development program (2016YFC0303406), Fundamental Research Funds for the Central University (HEUCFD1515, HEUCFM170113), Assembly Advanced Research Fund Of China (6140210020105), China Postdoctoral Science Foundation (2014M552661), Naval pre-research project, Ph.D. Student Research and Innovation Fund of the Fundamental Research Funds for the Central Universities (HEUGIP201801).

Conflict of interest: The authors declare that there is no conflict of interest regarding the publication of this paper.

References

Bambill, D.V., Rossit, C.A. and Felix, D.H. (2015), "Free vibrations of stepped axially functionally graded Timoshenko beams", *Meccanica*, **50**(4), 1073-1087. https://doi.org/10.1007/s11012-014-0053-4

Beni, Y.T., Mehralian, F. and Razavi, H. (2015), "Free vibration analysis of size-dependent shear deformable functionally graded cylindrical shell on the basis of modified couple stress theory", *Compos. Struct.*, **120**, 65-78. https://doi.org/10.1016/j.compstruct.2014.09.065

Bhrawy, A.H., Taha, T.M. and Machado, J.A.T. (2015), "A review of operational matrices and spectral techniques for fractional calculus", *Nonlinear Dyn.*, **81**(3), 1023-1052. https://doi.org/10.1007/s11071-015-2087-0

Bidgoli, M.R., Karimi, M.S. and Arani, A.G. (2015), "Viscous fluid induced vibration and instability of FG-CNT-reinforced cylindrical shells integrated with piezoelectric layers", *Steel Compos. Struct., Int. J.*, **19**(3), 713-733. https://doi.org/10.12989/scs.2015.19.3.713

Bodaghi, M. and Shakeri, M. (2012), "An analytical approach for free vibration and transient response of functionally graded piezoelectric cylindrical panels subjected to impulsive loads", *Compos. Struct.*, **94**(5), 1721-1735. https://doi.org/10.1016/j.compstruct.2012.01.009

Brischetto, S., Tornabene, F., Fantuzzi, N. and Viola, E. (2016), "3D exact and 2D generalized differential quadrature models for free vibration analysis of functionally graded plates and cylinders", *Meccanica*, **51**(9), 2059-2098. https://doi.org/10.1007/s11012-016-0361-y

Cao, Z.Y. and Tang, S.G. (2012), "Natural Vibration of Functionally Graded Cylindrical Shells With Infinite and Finite Lengths", *J. Vib. Acoust.*, **134**(1), 011013. https://doi.org/10.1115/1.4004900

Fantuzzi, N., Brischetto, S., Tornabene, F. and Viola, E. (2016), "2D and 3D shell models for the free vibration investigation of functionally graded cylindrical and spherical panels", *Compos. Struct.*, **154**, 573-590. https://doi.org/10.1016/j.compstruct.2016.07.076

Guo, J., Shi, D., Wang, Q., Tang, J. and Shuai, C. (2018), "Dynamic analysis of laminated doubly-curved shells with general boundary conditions by means of a domain decomposition method", *Int. J. Mech. Sci.*, **138**, 159-186. https://doi.org/10.1016/j.ijmecsci.2018.02.004

Hosseini-Hashemi, S., Ilkhani, M.R. and Fadaee, M. (2012), "Identification of the validity range of Donnell and Sanders shell theories using an exact vibration analysis of functionally graded thick cylindrical shell panel", *Acta Mechanica*, **223**(5), 1101-1118. https://doi.org/10.1007/s00707-011-0601-0

Hosseini-Hashemi, S., Derakhshani, M. and Fadaee, M. (2013), "An accurate mathematical study on the free vibration of stepped thickness circular/annular Mindlin functionally graded plates", *Appl. Math. Model.*, **37**(6), 4147-4164. https://doi.org/10.1007/s00707-011-0601-0

Javed, S., Viswanathan, K.K. and Aziz, Z.A. (2016), "Free vibration analysis of composite cylindrical shells with non-uniform thickness walls", *Steel Compos. Struct., Int. J.*, **20**(5), 1087-1102. https://doi.org/10.12989/scs.2016.20.5.1087

Jin, G.Y., Xie, X. and Liu, Z.G. (2014), "The Haar wavelet method for free vibration analysis of functionally graded cylindrical shells based on the shear deformation theory", *Compos. Struct.*, **108**, 435-448. https://doi.org/10.1016/j.compstruct.2013.09.044

Kamarian, S., Sadighi, M., Shakeri, M. and Yas, M.H. (2014), "Free vibration response of sandwich cylindrical shells with functionally graded material face sheets resting on Pasternak foundation", *J. Sandw. Struct. Mater.*, **16**(5), 511-533. https://doi.org/10.1177/1099636214541573

Kar, V.R. and Panda, S.K. (2015), "Nonlinear flexural vibration of shear deformable functionally graded spherical shell panel", *Steel Compos. Struct., Int. J.*, **18**(3), 693-709. https://doi.org/10.12989/scs.2015.18.3.693

Li, H., Pang, F., Gong, Q. and Teng, Y. (2019), "Free vibration analysis of axisymmetric functionally graded doubly-curved shells with un-uniform thickness distribution based on Ritz method", *Compos. Struct.*, **225**, 111145. https://doi.org/10.1016/j.compstruct.2019.111145

Liu, D.Y., Kitipornchai, S., Chen, W.Q. and Yang, J. (2018), "Three-dimensional buckling and free vibration analyses of initially stressed functionally graded graphene reinforced composite cylindrical shell", *Compos. Struct.*, **189**, 560-569. https://doi.org/10.1016/j.compstruct.2018.01.106

Pang, F., Li, H., Chen, H. and Shan, Y. (2019a), "Free vibration analysis of combined composite laminated cylindrical and spherical shells with arbitrary boundary conditions", *Mech. Adv. Mater. Struct.*, 1-18. https://doi.org/10.1080/15376494.2018.1553258

Pang, F., Li, H., Cui, J., Du, Y. and Gao, C. (2019b), "Application of flügge thin shell theory to the solution of free vibration behaviors for spherical-cylindrical-spherical shell: A unified formulation", *Eur. J. Mech. - A/Solids*, **74**, 381-393. https://doi.org/10.1016/j.euromechsol.2018.12.003

Pang, F.Z., Li, H.C., Jing, F.M. and Du, Y. (2019c), "Application of first-order shear deformation theory on vibration analysis of stepped functionally graded paraboloidal shell with general edge constraints", *Materials*, **12**(1), 69. https://doi.org/10.3390/ma12010069

Qu, Y., Chen, Y., Long, X., Hua, H. and Meng, G. (2013a), "Free and forced vibration analysis of uniform and stepped circular cylindrical shells using a domain decomposition method", *Appl. Acoust.*, **74**(3), 425-439. https://doi.org/10.1016/j.apacoust.2012.09.002

Qu, Y.G., Long, X.H., Yuan, G.Q. and Meng, G. (2013b), "A unified formulation for vibration analysis of functionally graded shells of revolution with arbitrary boundary conditions", *Compos. Part B-Eng.*, **50**, 381-402. https://doi.org/10.1016/j.compositesb.2013.02.028

Razavi, H., Babadi, A.F. and Beni, Y.T. (2017), "Free vibration analysis of functionally graded piezoelectric cylindrical nanoshell based on consistent couple stress theory", *Compos. Struct.*, **160**, 1299-1309. https://doi.org/10.1016/j.compstruct.2016.10.056

Su, Z., Jin, G.Y., Shi, S.X., Ye, T.G. and Jia, X.Z. (2014), "A unified solution for vibration analysis of functionally graded cylindrical, conical shells and annular plates with general boundary conditions", *Int. J. Mech. Sci.*, **80**, 62-80. https://doi.org/10.1016/j.ijmecsci.2014.01.002

Tang, D., Yao, X.L., Wu, G.X. and Peng, Y. (2017), "Free and forced vibration analysis of multi-stepped circular cylindrical shells with arbitrary boundary conditions by the method of reverberation-ray matrix", *Thin-Wall. Struct.*, **116**, 154-168. https://doi.org/10.1016/j.tws.2017.03.023

Tornabene, F. (2009), "Free vibration analysis of functionally graded conical, cylindrical shell and annular plate structures with a four-parameter power-law distribution", *Comput. Methods Appl. Mech. Eng.*, **198**(37-40), 2911-2935. https://doi.org/10.1016/j.cma.2009.04.011

Tornabene, F. and Viola, E. (2009), "Free vibration analysis of functionally graded panels and shells of revolution", *Meccanica*, **44**(3), 255-281. https://doi.org/10.1007/s11012-008-9167-x

Wang, Y.W. and Wu, D.F. (2017), "Free vibration of functionally graded porous cylindrical shell using a sinusoidal shear deformation theory", *Aerosp. Sci. Technol.*, **66**, 83-91. https://doi.org/10.1016/j.ast.2017.03.003

Wang, Q., Cui, X., Qin, B. and Liang, Q. (2017a), "Vibration analysis of the functionally graded carbon nanotube reinforced composite shallow shells with arbitrary boundary conditions", *Compos. Struct.*, **182**, 364-379. https://doi.org/10.1016/j.compstruct.2017.09.043

Wang, Q.S., Shi, D.Y., Liang, Q. and Pang, F.Z. (2017b), "Free vibration of moderately thick functionally graded parabolic and circular panels and shells of revolution with general boundary conditions", *Eng. Computat.*, **34**(5), 1598-1641. https://doi.org/10.1108/EC-06-2016-0218

Yas, M.H. and Aragh, B.S. (2011), "Elasticity solution for free vibration analysis of four-parameter functionally graded fiber orientation cylindrical panels using differential quadrature method", *Eur. J. Mech. A-Solids*, **30**(5), 631-638. https://doi.org/10.1016/j.euromechsol.2010.12.009

Yas, M.H., Pourasghar, A., Kamarian, S. and Heshmati, M. (2013), "Three-dimensional free vibration analysis of functionally graded nanocomposite cylindrical panels reinforced by carbon nanotube", *Mater. Des.*, **49**, 583-590. https://doi.org/10.1016/j.matdes.2013.01.001

Ye, T.G., Jin, G.Y. and Su, Z. (2016), "Three-dimensional vibration analysis of functionally graded sandwich deep open spherical and cylindrical shells with general restraints", *J. Vib. Control*, **22**(15), 3326-3354. https://doi.org/10.1177/1077546314553608

Zeighampour, H. and Shojaeian, M. (2017), "Size-dependent vibration of sandwich cylindrical nanoshells with functionally graded material based on the couple stress theory", *J. Brazil. Soc. Mech. Sci. Eng.*, **39**(7), 2789-2800. https://doi.org/10.1007/s40430-017-0770-4

Zghal, S., Frikha, A. and Dammak, F. (2018), "Free vibration analysis of carbon nanotube-reinforced functionally graded composite shell structures", *Appl. Math. Model.*, **53**, 132-155. https://doi.org/10.1016/j.apm.2017.08.021

Zhang, B., He, Y.M., Liu, D.B., Shen, L. and Lei, J.A. (2015), "Free vibration analysis of four-unknown shear deformable functionally graded cylindrical microshells based on the strain gradient elasticity theory", *Compos. Struct.*, **119**, 578-597. https://doi.org/10.1016/j.compstruct.2014.09.032

Zhao, X., Lee, Y.Y. and Liew, K.M. (2009), "Thermoelastic and vibration analysis of functionally graded cylindrical shells", *Int. J. Mech. Sci.*, **51**(9-10), 694-707. https://doi.org/10.1016/j.ijmecsci.2009.08.001

BU

Appendix A

The generalized mass and stiffness matrix of FG circular cylindrical shells used in Eq. (21) are given as

$$M = diag[M^1, M^2, \cdots, M^H] \tag{A1}$$

$$M^i = \int_{x_i}^{x_{i+1}} \int_0^{2\pi} \begin{bmatrix} M_{uu} & 0 & 0 & M_{ux} & 0 \\ 0 & M_{vv} & 0 & 0 & M_{v\theta} \\ 0 & 0 & M_{ww} & 0 & 0 \\ M_{ux} & 0 & 0 & M_{xx} & 0 \\ 0 & M_{v\theta} & 0 & 0 & M_{\theta\theta} \end{bmatrix} ABdxd\theta \tag{A2}$$

$$\begin{aligned} M_{uu} = I_0 U^T U,\ M_{vv} = I_0 V^T V,\ M_{ww} \\ = I_0 W^T W,\ M_{xx} = I_2 \Phi^T \Phi \end{aligned} \tag{A3}$$

$$M_{\theta\theta} = I_2 \Theta^T \Theta, M_{ux} = I_1 U^T \Phi, M_{v\theta} = I_1 V^T \Theta \tag{A4}$$

$$\begin{aligned} U = P_m \otimes C_n, \quad V = P_m \otimes S_n, \\ W = P_m \otimes C_n, \quad \Phi = P_m \otimes C_n, \quad \Theta = P_m \otimes S_n \end{aligned} \tag{A5}$$

$$P_m = [P_0^{(\alpha,\beta)}(\phi), P_1^{(\alpha,\beta)}(\phi), \cdots, P_m^{(\alpha,\beta)}(\phi), \cdots, P_M^{(\alpha,\beta)}(\phi)] \tag{A6}$$

$$C_n = [cos(0\theta), cos(1\theta), \cdots cos(n\theta), \cdots, cos(N\theta)] \tag{A7}$$

$$S_n = [sin(0\theta), sin(1\theta), \cdots sin(n\theta), \cdots, sin(N\theta)] \tag{A8}$$

$$K = K_\xi + K_b + K_s \tag{A9}$$

$$K_\xi = diag[K^1, K^2, \cdots, K^H] \tag{A10}$$

$$K^i = \int_{x_i}^{x_{i+1}} \int_0^{2\pi} \begin{bmatrix} K_{uu} & K_{uv} & K_{uw} & K_{ux} & K_{u\theta} \\ K_{uv}^T & K_{vv} & K_{vw} & K_{vx} & K_{v\theta} \\ K_{uw}^T & K_{vw}^T & K_{ww} & K_{wx} & K_{w\theta} \\ K_{ux}^T & K_{vx}^T & K_{wx}^T & K_{xx} & K_{x\theta} \\ K_{u\theta}^T & K_{v\theta}^T & K_{w\theta}^T & K_{x\theta}^T & K_{\theta\theta} \end{bmatrix} ABdxd\theta \tag{A11}$$

$$K_b = diag[K_{bl}, 0, \cdots, K_{br}] \tag{A12}$$

$$K_{bl} = \int_0^{2\pi} diag\left[K_{bl,uu}, K_{bl,vv}, K_{bl,ww}, K_{bl,xx}, K_{bl,\theta\theta}\right]_{x=x_0} Bd\theta \tag{A13}$$

$$K_{br} = \int_0^{2\pi} diag\left[K_{br,uu}, K_{br,vv}, K_{br,ww}, K_{br,xx}, K_{br,\theta\theta}\right]_{x=x_1} Bd\theta \tag{A14}$$

$$K_s = diag[K_s^1, K_s^2, \cdots, K_s^H] \tag{A15}$$

$$K_s^i = \int_0^{2\pi} \begin{bmatrix} K_{s0} & K_{s1} \\ K_{s1}^T & K_{s2} \end{bmatrix} Bd\theta \tag{A16}$$